
Plane four-node elements (without drilling rotation)

In this chapter, we describe techniques used to derive plane (2D) four-node elements with translational degrees of freedom, but without drilling rotations. Such elements are relatively simple so can be used to test the concepts which are later incorporated into either the 3D or shell elements.

The 2D elements can be directly used as a membrane part of the shell elements without drilling rotations, i.e. either in the shell elements with five dofs/node or in the “solid-shell” elements (without rotational dofs). However, the 2D elements are flat so for the warped shell elements, the formulation must be generalized as described in Sect. 14.

11.1 Basic equations

Consider the classical configuration space of the non-polar Cauchy continuum defined as $\mathcal{C} \doteq \{\boldsymbol{\chi}: B \rightarrow R^3\}$, where $\boldsymbol{\chi}$ is the deformation function defined on the reference configuration of the body B .

Basic functionals. The following functionals are used in this chapter:

1. The three-field Hu–Washizu (HW) functional.

A. For linear elastic materials, we can use the classical form of the HW functional

$$F_{\text{HW}}(\mathbf{u}, \boldsymbol{\sigma}, \boldsymbol{\varepsilon}) \doteq \int_B \{\mathcal{W}(\boldsymbol{\varepsilon}) + \boldsymbol{\sigma} \cdot [\mathbf{E}(\nabla \mathbf{u}) - \boldsymbol{\varepsilon}]\} dV - F_{\text{ext}}, \quad (11.1)$$

where $\mathcal{W}(\boldsymbol{\varepsilon})$ is the strain energy expressed by the independent strain $\boldsymbol{\varepsilon}$ and the stress $\boldsymbol{\sigma}$ plays the role of the Lagrange multiplier of the relation involving the independent strain $\boldsymbol{\varepsilon}$ and the Green strain

$\mathbf{E}(\mathbf{u})$, which is a function of the displacement \mathbf{u} . At the solution, we have $\boldsymbol{\varepsilon} = \mathbf{E}(\nabla\mathbf{u})$ and $\boldsymbol{\sigma} = \mathbf{S}$, where \mathbf{S} is the second Piola–Kirchhoff stress tensor. F_{ext} is the potential of the body force, the external loads, and the displacement boundary conditions.

B. For non-linear materials, the constitutive operator $\mathbb{C}(\boldsymbol{\varepsilon}) \doteq \partial^2\mathcal{W}(\boldsymbol{\varepsilon})/(\partial\boldsymbol{\varepsilon})^2$ depends on strain $\boldsymbol{\varepsilon}$ and we can use it only with increments. We write the displacements, stress, and strain in the incremental form

$$\mathbf{u}^i = \mathbf{u}^{i-1} + \Delta\mathbf{u}, \quad \boldsymbol{\sigma}^i = \boldsymbol{\sigma}^{i-1} + \Delta\boldsymbol{\sigma}, \quad \boldsymbol{\varepsilon}^i = \boldsymbol{\varepsilon}^{i-1} + \Delta\boldsymbol{\varepsilon}, \quad (11.2)$$

where $i, i-1$ are iteration indices and the increment $\Delta(\cdot) \doteq (\cdot)^i - (\cdot)^{i-1}$. Inserting these formulas into eq. (11.1), we obtain an incremental HW functional

$$F_{\text{HW}}^*(\Delta\mathbf{u}, \Delta\boldsymbol{\sigma}, \Delta\boldsymbol{\varepsilon}) \doteq \int_B \{ \mathcal{W}(\boldsymbol{\varepsilon} + \Delta\boldsymbol{\varepsilon}) + (\boldsymbol{\sigma} + \Delta\boldsymbol{\sigma}) \cdot [\mathbf{E}(\nabla(\mathbf{u} + \Delta\mathbf{u})) - (\boldsymbol{\varepsilon} + \Delta\boldsymbol{\varepsilon})] \} dV - F_{\text{ext}}, \quad (11.3)$$

where the index $(i-1)$ was omitted for clarity.

2. The two-field Hellinger–Reissner (HR) functional. A. For linear elastic materials, we can use the classical form of the HR functional

$$F_{\text{HR}}(\mathbf{u}, \boldsymbol{\sigma}) \doteq \int_B \left[-\frac{1}{2}\boldsymbol{\sigma} \cdot (\mathbb{C}^{-1}\boldsymbol{\sigma}) + \boldsymbol{\sigma} \cdot \mathbf{E}(\mathbf{u}) \right] dV - F_{\text{ext}}. \quad (11.4)$$

This functional is obtained as follows. For the linear elastic material, the strain energy is $\mathcal{W} \doteq \frac{1}{2}\boldsymbol{\varepsilon} \cdot (\mathbb{C}\boldsymbol{\varepsilon}) = \frac{1}{2}\boldsymbol{\varepsilon} \cdot \boldsymbol{\sigma}$, where \mathbb{C} is the constitutive operator. Then, using $\boldsymbol{\varepsilon} = \mathbb{C}^{-1}\boldsymbol{\sigma}$, we obtain

$$\mathcal{W} - \boldsymbol{\sigma} \cdot \boldsymbol{\varepsilon} = -\frac{1}{2}\boldsymbol{\sigma} \cdot \boldsymbol{\varepsilon} = -\frac{1}{2}\boldsymbol{\sigma} \cdot (\mathbb{C}^{-1}\boldsymbol{\sigma}).$$

By using this expression in the HW functional of eq. (11.1), we obtain the classical form of the HR functional of eq. (11.4).

B. For non-linear materials, the constitutive operator $\mathbb{C}(\boldsymbol{\varepsilon}) \doteq \partial^2\mathcal{W}(\boldsymbol{\varepsilon})/(\partial\boldsymbol{\varepsilon})^2$ depends on strain $\boldsymbol{\varepsilon}$ and we can use it only with increments. We write the displacements, stress, and strain in the incremental form

$$\mathbf{u}^i = \mathbf{u}^{i-1} + \Delta\mathbf{u}, \quad \boldsymbol{\sigma}^i = \boldsymbol{\sigma}^{i-1} + \Delta\boldsymbol{\sigma}, \quad \boldsymbol{\varepsilon}^i = \boldsymbol{\varepsilon}^{i-1} + \Delta\boldsymbol{\varepsilon}, \quad (11.5)$$

where $i, i-1$ are iteration indices and the increment $\Delta(\cdot) \doteq (\cdot)^i - (\cdot)^{i-1}$. The strain increment is expressed by an inverse constitutive equation

$$\Delta\boldsymbol{\varepsilon} = (\mathbb{C}^{i-1})^{-1} \Delta\boldsymbol{\sigma}, \quad \mathbb{C}^{i-1} \doteq \mathbb{C}(\boldsymbol{\varepsilon}^{i-1}). \quad (11.6)$$

Inserting these formulas into the Hu–Washizu functional of eq. (11.1), we obtain an incremental HR functional

$$F_{\text{HR}}^*(\Delta\mathbf{u}, \Delta\boldsymbol{\sigma}) \doteq \int_B \{ \mathcal{W}(\boldsymbol{\varepsilon} + \mathbb{C}^{-1} \Delta\boldsymbol{\sigma}) - (\boldsymbol{\sigma} + \Delta\boldsymbol{\sigma}) \cdot [\boldsymbol{\varepsilon} + \mathbb{C}^{-1} \Delta\boldsymbol{\sigma} - \mathbf{E}(\mathbf{u} + \Delta\mathbf{u})] \} dV - F_{\text{ext}}, \quad (11.7)$$

where the index $(i-1)$ was omitted for clarity. This functional depends on two fields, similarly as in the classical HR functional of eq. (11.4). The values from the previous $(i-1)$ th iteration, i.e. \mathbf{u} , $\boldsymbol{\sigma}$ and $\boldsymbol{\varepsilon}$, must be stored as history variables.

3. The potential energy (PE) functional.

$$F_{\text{PE}}(\mathbf{u}) \doteq \int_B \mathcal{W}(\mathbf{u}) dV - F_{\text{ext}}, \quad (11.8)$$

where $\mathcal{W}(\mathbf{u})$ is the strain energy expressed by displacements \mathbf{u} . This functional is obtained from eq. (11.1) assuming that $\boldsymbol{\varepsilon} = \mathbf{E}(\mathbf{u})$, for which the term with stress vanishes. Then $\mathcal{W}(\boldsymbol{\varepsilon}) = \mathcal{W}(\mathbf{E}(\mathbf{u})) = \mathcal{W}(\mathbf{u})$.

These three functionals form the basis of the elements developed in the next sections.

Strain energy and constitutive equation. Assume that the strain energy density \mathcal{W} , defined per unit non-deformed volume, is a function of the right Cauchy–Green deformation tensor $\mathbf{C} \doteq \mathbf{F}^T \mathbf{F}$, where \mathbf{F} is the deformation gradient, so that the objectivity requirement is satisfied. The constitutive law for the second Piola–Kirchhoff stress \mathbf{S} is as follows:

$$\mathbf{S} = 2 \partial_{\mathbf{C}} \mathcal{W}(\mathbf{C}). \quad (11.9)$$

The work conjugate to \mathbf{S} is the Green strain $\mathbf{E} \doteq \frac{1}{2}(\mathbf{C} - \mathbf{I})$. The constitutive tangent operator is defined as $\mathbb{C} \doteq \partial \mathbf{S} / \partial \mathbf{E} = \partial^2 \mathcal{W}(\mathbf{E}) / (\partial \mathbf{E})^2$.

The two-dimensional (2D) incremental constitutive equations and the constitutive operator can be obtained by applying the plane stress condition to the incremental constitutive equation written for 3D strains and stresses, see Sect. 7.2.1.

Natural basis at the element's center. The position vector in the initial configuration is approximated as

$$\mathbf{y}(\xi, \eta) = \sum_{I=1}^4 N_I(\xi, \eta) \mathbf{y}_I, \quad (11.10)$$

where $N_I(\xi, \eta)$ are the bilinear shape functions of eq. (10.3) and $\xi, \eta \in [-1, +1]$ are natural coordinates.

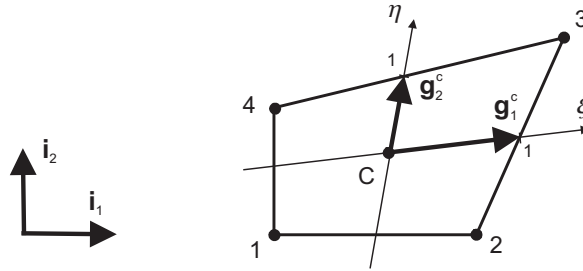


Fig. 11.1 Natural basis at the element's center $\{\mathbf{g}_k^c\}$ and the reference basis $\{\mathbf{i}_k\}$.

The vectors of the natural basis are defined as in eq. (10.15),

$$\mathbf{g}_1(\xi, \eta) \doteq \frac{\partial \mathbf{y}(\xi, \eta)}{\partial \xi}, \quad \mathbf{g}_2(\xi, \eta) \doteq \frac{\partial \mathbf{y}(\xi, \eta)}{\partial \eta}, \quad (11.11)$$

and the vectors of the natural basis at the element's center, i.e. $\{\mathbf{g}_k^c\}$ ($k = 1, 2$), are defined as

$$\mathbf{g}_1^c \doteq \mathbf{g}_1|_{\xi, \eta=0}, \quad \mathbf{g}_2^c \doteq \mathbf{g}_2|_{\xi, \eta=0}. \quad (11.12)$$

In general, \mathbf{g}_1^c and \mathbf{g}_2^c are neither unit nor orthogonal, see Fig. 11.1. The co-basis vectors \mathbf{g}_c^k are defined as in eq. (10.47), by the relation $\mathbf{g}_c^k \cdot \mathbf{g}_l^c = \delta_l^k$ ($l = 1, 2$).

In the reference Cartesian basis $\{\mathbf{i}_k\}$, we have $\mathbf{y} = x\mathbf{i}_1 + y\mathbf{i}_2$, and the global Jacobian matrix is

$$\mathbf{J} \doteq \begin{bmatrix} \frac{\partial x}{\partial \xi} & \frac{\partial x}{\partial \eta} \\ \frac{\partial y}{\partial \xi} & \frac{\partial y}{\partial \eta} \end{bmatrix} = \begin{bmatrix} \mathbf{g}_1 \cdot \mathbf{i}_1 & \mathbf{g}_2 \cdot \mathbf{i}_1 \\ \mathbf{g}_1 \cdot \mathbf{i}_2 & \mathbf{g}_2 \cdot \mathbf{i}_2 \end{bmatrix}, \quad (11.13)$$

where $\mathbf{g}_1, \mathbf{g}_2$ are the vectors of the natural basis of eq. (11.11).

11.2 Displacement element Q4

The basic four-node element derived from the PE functional for displacements approximated by bilinear shape functions, is designated as Q4. The displacements preserve inter-element continuity, i.e. are compatible, and the neighboring elements are congruent (conform). However, accuracy of Q4 is so poor that is of no practical importance.

Compatible displacements, deformation gradient and Green strain. The position vector in the initial configuration and the compatible displacements for the four-node quadrilateral are approximated as

$$\mathbf{y}(\xi, \eta) = \sum_{I=1}^4 N_I(\xi, \eta) \mathbf{y}_I, \quad \mathbf{u}^c(\xi, \eta) = \sum_{I=1}^4 N_I(\xi, \eta) \mathbf{u}_I, \quad (11.14)$$

where $N_I(\xi, \eta) \doteq \frac{1}{4}(1 + \xi_I \xi)(1 + \eta_I \eta)$ are the bilinear shape functions, $\xi, \eta \in [-1, +1]$ are natural coordinates and I designates the corner nodes. The deformation gradient is defined as

$$\mathbf{F}^c = \frac{\partial(\mathbf{y} + \mathbf{u}^c)}{\partial \boldsymbol{\xi}} \frac{\partial \boldsymbol{\xi}}{\partial \mathbf{y}} = \mathbf{F}_\xi \mathbf{J}^{-1}, \quad (11.15)$$

where $\mathbf{F}_\xi \doteq \partial(\mathbf{y} + \mathbf{u}^c)/\partial \boldsymbol{\xi}$, $\mathbf{J} \doteq \partial \mathbf{y}/\partial \boldsymbol{\xi}$ is the Jacobian matrix and $\boldsymbol{\xi} \doteq [\xi, \eta]^T$. Then the compatible Green strain in the global frame is

$$\mathbf{E}^c = \frac{1}{2}(\mathbf{F}^{cT} \mathbf{F}^c - \mathbf{I}) = \frac{1}{2}[\mathbf{J}^{-T}(\mathbf{F}_\xi^T \mathbf{F}_\xi) \mathbf{J}^{-1} - \mathbf{I}]. \quad (11.16)$$

The vectors and matrices of components used above are expressed in the global reference basis $\{\mathbf{i}_k\}$.

Global and local forms of deformation gradient and Green strain. Below, vectors and matrices of components are considered and the index “ G ” indicates that the components are in the global reference basis, while “ L ” indicates that they are in the local Cartesian basis at the element’s center. Define the local position vectors and the local displacements as follows:

$$\mathbf{y}_L \doteq \mathbf{R}_{0c}^T \mathbf{y}_G, \quad \mathbf{u}_L^c \doteq \mathbf{R}_{0c}^T \mathbf{u}_G^c, \quad (11.17)$$

where $\mathbf{R}_{0c} \in \text{SO}(3)$ defines the position of the local frame in the global reference frame. Then,

$$\mathbf{J}_G \doteq \frac{\partial \mathbf{y}_G}{\partial \boldsymbol{\xi}} = \frac{\partial (\mathbf{R}_{0c} \mathbf{y}_L)}{\partial \boldsymbol{\xi}} = \mathbf{R}_{0c} \frac{\partial \mathbf{y}_L}{\partial \boldsymbol{\xi}} = \mathbf{R}_{0c} \mathbf{J}_L,$$

$$\frac{\partial (\mathbf{y}_G + \mathbf{u}_G^c)}{\partial \boldsymbol{\xi}} = \mathbf{R}_{0c} \frac{\partial (\mathbf{y}_L + \mathbf{u}_L^c)}{\partial \boldsymbol{\xi}}$$

and the deformation gradient can be expressed as

$$\mathbf{F}_G^c = \frac{\partial (\mathbf{y}_G + \mathbf{u}_G^c)}{\partial \boldsymbol{\xi}} \frac{\partial \boldsymbol{\xi}}{\partial \mathbf{y}_G} = \mathbf{R}_{0c} \mathbf{F}_L^c \mathbf{R}_{0c}^T, \quad (11.18)$$

where

$$\mathbf{F}_L^c \doteq \frac{\partial (\mathbf{y}_L + \mathbf{u}_L^c)}{\partial \boldsymbol{\xi}} \mathbf{J}_L^{-1} \quad (11.19)$$

is the local form of the deformation gradient. In a similar manner, the Green strain can be expressed as

$$\mathbf{E}_G^c \doteq \frac{1}{2} [\mathbf{F}_G^{cT} \mathbf{F}_G^c - \mathbf{I}] = \frac{1}{2} [\mathbf{R}_{0c}^T (\mathbf{F}_L^c)^T \mathbf{F}_L^c \mathbf{R}_{0c} - \mathbf{I}] = \mathbf{R}_{0c}^T \mathbf{E}_L^c \mathbf{R}_{0c}, \quad (11.20)$$

where

$$\mathbf{E}_L^c \doteq \frac{1}{2} [(\mathbf{F}_L^c)^T \mathbf{F}_L^c - \mathbf{I}] \quad (11.21)$$

is the local form of the Green strain. The local \mathbf{F}_L^c and \mathbf{E}_L^c can be used to derive the local tangent matrix and the residual vector, which is more convenient. Afterwards, the matrix and the vector must be rotated to the global basis.

Approximation of strains in Q4. The bilinear approximations of displacement components can be written as

$$u(\xi, \eta) = u_0 + \xi u_1 + \eta u_2 + \xi \eta u_3, \quad v(\xi, \eta) = v_0 + \xi v_1 + \eta v_2 + \xi \eta v_3, \quad (11.22)$$

where $\xi, \eta \in [-1, +1]$ and the coefficients u_i and v_i ($i = 0, 1, 2, 3$) are functions of the nodal displacement components.

Consider a bi-unit (2×2) square element, for which the position vector components are $x = \xi$ and $y = \eta$, and the Jacobian matrix is the identity matrix. Then we have the following approximations:

- the displacement gradient,

$$\nabla \mathbf{u} \doteq \begin{bmatrix} u_{,\xi} & u_{,\eta} \\ v_{,\xi} & v_{,\eta} \end{bmatrix} = \begin{bmatrix} u_1 + \eta u_3 & u_2 + \xi u_3 \\ v_1 + \eta v_3 & v_2 + \xi v_3 \end{bmatrix}, \quad (11.23)$$

- the linear strain,

$$\boldsymbol{\varepsilon} \doteq \text{sym} \nabla \mathbf{u} = \begin{bmatrix} u_1 + \eta u_3 & \frac{1}{2}[(u_2 + v_1) + \xi u_3 + \eta v_3] \\ \text{sym.} & v_2 + \xi v_3 \end{bmatrix}. \quad (11.24)$$

We see that ε_{11} and ε_{22} are incomplete linear polynomials of ξ and η , while the shear strain ε_{12} is a complete linear polynomial.

Despite the completeness of ε_{12} , the Q4 element performs poorly in tests involving shear strains. When ε_{12} is calculated (sampled) only at the element center and this value is used to approximate the whole field within the element, i.e.

$$\varepsilon_{12}(\xi, \eta) \approx (\varepsilon_{12})_c, \quad (11.25)$$

then the element still has a correct rank and the results are improved, see numerical results for the AS12 element in [256]. This feature leads to the concept of the “one-integration point” elements. The accuracy of the AS12 element is worse than of the elements discussed in the next sections.



Fig. 11.2 Pure bending: a) exact deformation, b) deformation of Q4 element.

Another observation made in [248] is that the quadratic terms are missing in eq. (11.22), so pure bending of the element cannot be properly represented, see Fig. 11.2.

11.3 Solution of FE equations for problems with additional variables

Improved formulations of four-node element. A lot of research has been devoted to improving the formulation of a four-node element and two directions were taken:

1. approximations of strains were enhanced, leading to the *enhanced strain* methods, see Sect. 11.4. The stress was eliminated from these formulations.

2. Mixed HR and HW functionals were applied instead of the PE functional, leading to the *mixed* methods, see Sect. 11.5. The stress was retained in these formulations.

Both these directions are combined by the mixed/enhanced methods.

Set of equations for problems with additional variables. For the considered classes of methods, the governing functional F depends on two sets of variables: the nodal displacements \mathbf{u}_I and the elemental multipliers \mathbf{q} .

For kinematically non-linear problems, the stationarity condition of $F(\mathbf{u}_I, \mathbf{q})$ yields a system of equilibrium equations for an element,

$$\mathbf{r}_u \doteq \frac{\partial F(\mathbf{u}_I, \mathbf{q})}{\partial \mathbf{u}_I} = \mathbf{0}, \quad \mathbf{r}_q \doteq \frac{\partial F(\mathbf{u}_I, \mathbf{q})}{\partial \mathbf{q}} = \mathbf{0}. \quad (11.26)$$

The linearized (Newton) form of these equations is as follows:

$$\begin{bmatrix} \mathbf{K} & \mathbf{L} \\ \mathbf{L}^T & \mathbf{K}_{qq} \end{bmatrix} \begin{bmatrix} \Delta \mathbf{u}_I \\ \Delta \mathbf{q} \end{bmatrix} = - \begin{bmatrix} \mathbf{r}_u \\ \mathbf{r}_q \end{bmatrix}, \quad (11.27)$$

where

$$\mathbf{K} \doteq \frac{\partial \mathbf{r}_u}{\partial \mathbf{u}_I}, \quad \mathbf{L} \doteq \frac{\partial \mathbf{r}_u}{\partial \mathbf{q}}, \quad \mathbf{K}_{qq} \doteq \frac{\partial \mathbf{r}_q}{\partial \mathbf{q}}. \quad (11.28)$$

To eliminate $\Delta \mathbf{q}$ at the element level, we calculate it from the second of eq. (11.27) as follows:

$$\Delta \mathbf{q} = -\mathbf{K}_{qq}^{-1}(\mathbf{r}_q + \mathbf{L}^T \Delta \mathbf{u}_I) \quad (11.29)$$

and, next, we use it in the first equation, which yields

$$\mathbf{K}^* \Delta \mathbf{u}_I = -\mathbf{r}^*, \quad (11.30)$$

where

$$\mathbf{K}^* \doteq \mathbf{K} - \mathbf{L} \mathbf{K}_{qq}^{-1} \mathbf{L}^T, \quad \mathbf{r}^* \doteq \mathbf{r}_u - \mathbf{L} \mathbf{K}_{qq}^{-1} \mathbf{r}_q. \quad (11.31)$$

Subsequently, \mathbf{K}^* and \mathbf{r}^* are aggregated for all elements and the global set of equations is solved for $\Delta \mathbf{u}_I$. Then we update the nodal displacements $\mathbf{u}_I = \mathbf{u}_I + \Delta \mathbf{u}_I$. The elemental multipliers \mathbf{q} are treated as described below.

Remark. Note that the system of equations (11.27) written for all elements is solvable if the matrix \mathbf{K}_{qq} for each element and the matrix \mathbf{K}^* for all elements additionally modified by boundary conditions, are invertible. Note that eigenvalues of the non-reduced tangent matrix of eq. (11.27) are different from those of matrix \mathbf{K}^* of eq. (11.30).

Schemes of update of multipliers. Several update schemes of the vector of multipliers can be developed and each requires specific storage and implementation. We have implemented and tested two update schemes; in both, the update $\mathbf{q} = \mathbf{q} + \Delta\mathbf{q}$ is local, i.e. it is performed in each element separately.

Scheme U1. In this scheme, the storage space is minimal, as we store only one vector \mathbf{q} . For the iteration i , we use eq. (11.29) in the following form:

$$(\Delta\mathbf{q})^i = -\mathbf{K}_{qq}^{-1} (\mathbf{r}_q + \mathbf{L}^T \Delta\mathbf{u}_I^{i-1}), \quad \mathbf{q}^i = \mathbf{q}^{i-1} + (\Delta\mathbf{q})^i, \quad (11.32)$$

where \mathbf{K}_{qq} , \mathbf{r}_q and \mathbf{L} are calculated for $(\mathbf{u}_I^{i-1}, \mathbf{q}^{i-1})$. This update is performed just after the local matrices have been generated and the updated \mathbf{q}^i is stored. Note that so-updated multipliers are not used until the next iteration, $i + 1$, and \mathbf{q}^i is obtained for $\Delta\mathbf{u}_I^{i-1}$, so the difference is of two iterations!

We tested that this scheme performs better (less often causes divergence) if the update is performed only in the first iteration of each step. (For the convergent solution of the previous step, $\Delta\mathbf{u}_I^{i-1} \approx \mathbf{0}$, and then we can omit the last term in the above equation.)

Scheme U2. This scheme is more exact than the previous one because it uses the last increment $\Delta\mathbf{u}_I^i$, but requires more storage. It is equivalent to the one globally treating \mathbf{q} , in the same way as \mathbf{u}_I , instead of eliminating it at the element's level. The advantage of the scheme U2 over such a global treatment is that to invert \mathbf{K}_{qq} , we can use a specialized solver and retain an effective band-profile solver for the global equations. Let us rewrite eq. (11.29) as follows:

$$\Delta\mathbf{q} = -\underbrace{\mathbf{K}_{qq}^{-1} \mathbf{r}_q}_{\doteq \mathbf{v}} + \underbrace{\mathbf{K}_{qq}^{-1} \mathbf{L}^T}_{\doteq \mathbf{A}} \Delta\mathbf{u}_I, \quad (11.33)$$

where \mathbf{v} and \mathbf{A} are updated and stored. Hence, we have to store vectors \mathbf{q} and \mathbf{v} of dimension nM , and a matrix \mathbf{A} of dimension $nM \times nst$, where nM is a number of additional modes and nst is a number of dofs/element ($nst = 8$ for four-node element with two dofs/node). The update is performed before the local matrices are generated, as follows:

1. retrieve \mathbf{v} and \mathbf{A} ,
2. calculate

$$(\Delta \mathbf{q})^i = -\mathbf{v} + \mathbf{A} \Delta \mathbf{u}_I^{i-1}, \quad \mathbf{q}^i = \mathbf{q}^{i-1} + (\Delta \mathbf{q})^i, \quad (11.34)$$

for the last available $\Delta \mathbf{u}_I^{i-1}$,

3. generate the local elemental matrices and vectors.

As a by-product of step 3, we obtain the updated \mathbf{v} and \mathbf{A} , which we store for the next step.

The convergence rate for both these schemes is compared in [256, 257], for the slender cantilever example of Sect.15.3.1. The scheme U1 performs reasonably well only for the enhanced strain elements; the use of scheme U2 appears to be crucial for mixed elements.

Remark. Finally, we mention that the matrix \mathbf{K}_{qq} is symmetric and sparse and we can use these properties to effectively compute its inverse. Besides, we note that to find \mathbf{q}_i , we can use another approach and directly solve the set of equations $\mathbf{r}_q = \mathbf{0}$ for fixed \mathbf{u}_I . This can be a useful approach, e.g., in dynamics and an explicit time-integration scheme.

11.4 Enhanced strain elements based on potential energy

The class of the enhanced strain methods is based on the technique of adding additional terms either to displacements, or strains, or the displacement gradient, with the purpose of improving the element's performance.

In all the methods described below, the multipliers \mathbf{q} are associated with the element (not with the nodes) and are eliminated (condensed out) on the element level. They are discontinuous across the element boundaries.

11.4.1 ID4 element

The incompatible displacements (ID) method was proposed in [248] to improve the behavior of the Q4 element in pure bending, see Fig. 11.2. Later, it was discovered that the ID element does not pass the patch test for distorted meshes and a correction was proposed in [234]. From today’s perspective, the idea of the ID method was ingenious and the whole class of the enhanced strain methods stems from it.

In the ID method, the assumed incompatible displacements are added to the compatible ones as follows:

$$\underbrace{\mathbf{u}(\xi, \eta)}_{\text{enhanced}} \doteq \underbrace{\mathbf{u}^c(\xi, \eta)}_{\text{compatible}} + \underbrace{\mathbf{u}^{\text{inc}}(\xi, \eta)}_{\text{incompatible}}. \quad (11.35)$$

Original formulation. In the original paper, the incompatible displacements are assumed in the following form:

$$\mathbf{u}^{\text{inc}}(\xi, \eta) \doteq \mathbf{i}_1 u^{\text{inc}}(\xi, \eta) + \mathbf{i}_2 v^{\text{inc}}(\xi, \eta), \quad (11.36)$$

where

$$\begin{bmatrix} u^{\text{inc}}(\xi, \eta) \\ v^{\text{inc}}(\xi, \eta) \end{bmatrix} \doteq \begin{bmatrix} q_1 P_1(\xi) + q_3 P_2(\eta) \\ q_2 P_1(\xi) + q_4 P_2(\eta) \end{bmatrix}. \quad (11.37)$$

and the quadratic (bubble) modes $P_1(\xi) \doteq 1 - \xi^2$ and $P_2(\eta) \doteq 1 - \eta^2$. Four multipliers q_i are used, see Fig. 11.3. The incompatible displacements are assumed in the Cartesian basis $\{\mathbf{i}_k\}$, similarly to the compatible displacements.

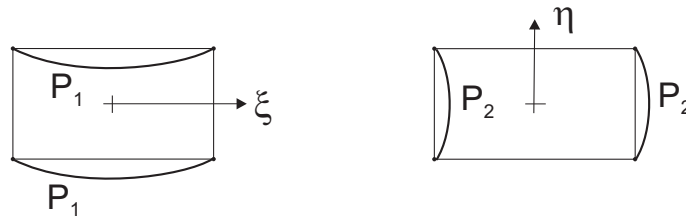


Fig. 11.3 Incompatible modes P_1 and P_2 .

The effect of introducing the incompatible displacements can be shown as follows. Consider a bi-unit (2×2) square element, for which the position

vector components are $x = \xi$ and $y = \eta$ and the Jacobian matrix is the identity matrix. Then, for the incompatible displacements, we obtain

- the “incompatible” displacement gradient,

$$\nabla \mathbf{u}^{\text{inc}} \doteq \begin{bmatrix} u_{,\xi}^{\text{inc}} & u_{,\eta}^{\text{inc}} \\ v_{,\xi}^{\text{inc}} & v_{,\eta}^{\text{inc}} \end{bmatrix} = -2 \begin{bmatrix} q_1 \xi & q_3 \eta \\ q_2 \xi & q_4 \eta \end{bmatrix}, \quad (11.38)$$

- the “incompatible” linear strain,

$$\boldsymbol{\varepsilon}^{\text{inc}} \doteq \text{sym} \nabla \mathbf{u}^{\text{inc}} = -2 \begin{bmatrix} q_1 \xi & \frac{1}{2}(q_2 \xi + q_3 \eta) \\ \text{sym.} & q_4 \eta \end{bmatrix}. \quad (11.39)$$

Note that $\varepsilon_{11}^{\text{inc}}$ and $\varepsilon_{22}^{\text{inc}}$ of (11.39) enhance the compatible ε_{11} and ε_{22} of eq. (11.24), so these components become complete linear polynomials. The role of the shear component $\varepsilon_{12}^{\text{inc}}$ is different; it rather de-enhances the compatible ε_{12} , in which the ξ and η terms were already present. Nonetheless, this de-enhancement is beneficial and significantly improves accuracy in tests involving the in-plane shear. It is more effective than the sampling of ε_{12} at the element’s center of eq. (11.25).

Modified formulation. Element ID4. We can define the incompatible displacements in the natural basis at the element’s center $\{\mathbf{g}_k^c\}$ of Fig. 11.1,

$$\mathbf{u}^{\text{inc}}(\xi, \eta) \doteq \mathbf{g}_1^c u^{\text{inc}}(\xi, \eta) + \mathbf{g}_2^c v^{\text{inc}}(\xi, \eta), \quad (11.40)$$

which can be rewritten as

$$\begin{bmatrix} u_C^{\text{inc}} \\ v_C^{\text{inc}} \end{bmatrix} = \mathbf{J}_c \begin{bmatrix} u^{\text{inc}} \\ v^{\text{inc}} \end{bmatrix}, \quad (11.41)$$

where \mathbf{J}_c is the Jacobian matrix of eq. (11.13) at the element’s center, and $u_C^{\text{inc}}, v_C^{\text{inc}}$ are the components in the Cartesian basis $\{\mathbf{i}_k\}$. The last form is obtained by using $\mathbf{g}_1^c = (\mathbf{g}_1^c \cdot \mathbf{i}_1)\mathbf{i}_1 + (\mathbf{g}_1^c \cdot \mathbf{i}_2)\mathbf{i}_2$ and $\mathbf{g}_2^c = (\mathbf{g}_2^c \cdot \mathbf{i}_1)\mathbf{i}_1 + (\mathbf{g}_2^c \cdot \mathbf{i}_2)\mathbf{i}_2$, by separation of terms multiplied by \mathbf{i}_1 and \mathbf{i}_2 .

The discrete F_{PE} functional depends on two sets of variables: the nodal displacements \mathbf{u}_I and the elemental multipliers \mathbf{q} of the incompatible displacement modes. The obtained set of FE equations is given by eq. (11.27) and to update the stress multipliers, the scheme U2 of eq. (11.34) should be used.

Variational basis of the ID method. We can write the PE functional of eq. (11.8) for the enhanced displacements,

$$F_{\text{PE}}(\mathbf{u}^{\text{enh}}) \doteq \int_B \mathcal{W}(\mathbf{u}^{\text{enh}}) \, dV - F_{\text{ext}}, \quad (11.42)$$

on use of eqs. (11.35) and (11.40), which furnishes a general formula. The original ID method was developed for small strains and the SVK material, for which the strain energy can be written as

$$\mathcal{W}(\mathbf{u}^{\text{enh}}) \doteq \frac{1}{2} \int_B (\boldsymbol{\varepsilon}_v^c + \boldsymbol{\varepsilon}_v^{\text{inc}})^T \mathbb{C} (\boldsymbol{\varepsilon}_v^c + \boldsymbol{\varepsilon}_v^{\text{inc}}) \, dV, \quad (11.43)$$

where $\boldsymbol{\varepsilon}_v^c \doteq \boldsymbol{\varepsilon}_v(\mathbf{u}^c)$, $\boldsymbol{\varepsilon}_v^{\text{inc}} \doteq \boldsymbol{\varepsilon}_v(\mathbf{u}^{\text{inc}})$. Here, $(\cdot)_v$ denotes a vector of tensorial components. The obtained set of FE equations has the structure given by eq. (11.27), where

$$\begin{aligned} \mathbf{K} &\doteq \int_B \mathbf{B}^T \mathbb{C} \mathbf{B} \, dV, & \mathbf{L} &\doteq \int_B \mathbf{B}^T \mathbb{C} \mathbf{G} \, dV, & \mathbf{K}_{qq} &\doteq \int_B \mathbf{G}^T \mathbb{C} \mathbf{G} \, dV, \\ \mathbf{r}_u &= -\mathbf{p}, & \mathbf{r}_q &= \mathbf{0}. \end{aligned} \quad (11.44)$$

The tangent operators are defined as

$$\mathbf{B} \doteq \partial \boldsymbol{\varepsilon}_v^c / \partial \mathbf{u}_I, \quad \mathbf{G} \doteq \partial \boldsymbol{\varepsilon}_v^{\text{inc}} / \partial \mathbf{q}, \quad (11.45)$$

where \mathbf{B} is for compatible strains, while \mathbf{G} for incompatible strains. Besides, \mathbf{p} is the vector of external loads.

The stress for the linear material is obtained in the ID method as follows:

$$\boldsymbol{\sigma}_v^{\text{enh}} \doteq \partial \mathcal{W}(\mathbf{u}^{\text{enh}}) / \partial \boldsymbol{\varepsilon}_v^{\text{enh}} = \mathbb{C} (\boldsymbol{\varepsilon}_v^c + \boldsymbol{\varepsilon}_v^{\text{inc}}). \quad (11.46)$$

Sufficient condition to pass the patch test. The incompatible modes are quadratic functions and yield the incompatible strains which are linear, see eq. (11.39). Hence, these modes should not be activated in the patch test, in which the strains are constant. This leads to the requirement that the formulation of the ID element should yield $\mathbf{q} = \mathbf{0}$ in this test and, generally, for any nodal displacements \mathbf{u}_I generating constant strains.

It can be shown that to obtain $\mathbf{q} = \mathbf{0}$ in the constant strain patch test, it suffices to satisfy the condition

$$\int_B \mathbf{G} \, dV = \mathbf{0}, \quad (11.47)$$

by the reasoning of [234], which we outline below. From the second of eq. (11.27), we can calculate

$$\mathbf{q} = -\mathbf{K}_{qq}^{-1} \mathbf{L}^T \mathbf{u}_I. \quad (11.48)$$

To obtain $\mathbf{q} = \mathbf{0}$, we may require the condition $\mathbf{L}^T \mathbf{u}_I = \mathbf{0}$ to be satisfied. By the definition of \mathbf{L} of eq. (11.44),

$$\mathbf{L}^T \mathbf{u}_I = \int_B \mathbf{G}^T (\mathbb{C} \mathbf{B} \mathbf{u}_I) dV = \int_B \mathbf{G}^T \boldsymbol{\sigma} dV, \quad (11.49)$$

where $\boldsymbol{\sigma} \doteq \mathbb{C}(\mathbf{B} \mathbf{u}_I)$ is the stress, as $\mathbf{B} \mathbf{u}_I$ is the strain in a kinematically linear problem. In the patch test, the nodal displacements yield a constant strain and, hence, for a constant \mathbb{C} , also the stress $\boldsymbol{\sigma}$ is constant and can be taken away from under the integral, which yields the condition of eq. (11.47). This condition is enough to yield $\mathbf{L}^T \mathbf{u}_I = \mathbf{0}$, $\mathbf{q} = -\mathbf{K}_{qq}^{-1} \mathbf{L}^T \mathbf{u}_I = \mathbf{0}$, and to pass the constant strain patch test.

The original version of the ID method of [248], based on eq. (11.36), did not pass the patch test for elements of distorted initial geometry (non-parallelograms) and was subsequently corrected in [234] by using the Jacobian matrix at the element's center and the modified Jacobian inverse, see eq. (11.50). In the modified version of the ID method of eq. (11.41), only the second of these corrections is necessary because the \mathbf{J}_c is present as a natural consequence of the use of $\{\mathbf{g}_k^c\}$.

Modification of the Jacobian inverse. The Jacobian inverse \mathbf{J}^{-1} varies over the element area. To eliminate the dependence of it on ξ, η , we may define

$$(\mathbf{J}^{-1})^* \doteq \mathbf{J}_c^{-1} \left(\frac{j_c}{j} \right), \quad (11.50)$$

where $j \doteq \det \mathbf{J}$, and the subscript c indicates the value at the element's center. The 2×2 -point Gauss integration of $(\mathbf{J}^{-1})^*$ yields

$$\int_A (\mathbf{J}^{-1})^* dA = \sum_{g=1}^4 (\mathbf{J}^{-1})_g^* j_g = 4 \mathbf{J}_c^{-1} j_c, \quad (11.51)$$

which is exactly the result of the 1-point integration of \mathbf{J}^{-1} . Here, g is the index of integration points.

Displacement gradient for incompatible displacements. The displacement gradient can be split into a compatible and incompatible part,

$$\nabla \mathbf{u} = \left[\frac{\partial(\mathbf{u}^c + \mathbf{u}^{\text{inc}})}{\partial \xi} \right] \mathbf{J}^{-1} = \left[\frac{\partial \mathbf{u}^c}{\partial \xi} \right] \mathbf{J}^{-1} + \underline{\left[\frac{\partial \mathbf{u}^{\text{inc}}}{\partial \xi} \right] \mathbf{J}^{-1}}. \quad (11.52)$$

The incompatible (underlined) part is evaluated at the Gauss point g by using the incompatible displacements of eq. (11.41) and the modified inverse Jacobian of eq. (11.50),

$$\nabla \mathbf{u}_g^{\text{inc}} = \mathbf{J}_c \begin{bmatrix} \frac{\partial u^{\text{inc}}}{\partial \xi} & \frac{\partial u^{\text{inc}}}{\partial \eta} \\ \frac{\partial v^{\text{inc}}}{\partial \xi} & \frac{\partial v^{\text{inc}}}{\partial \eta} \end{bmatrix}_g \mathbf{J}_c^{-1} \begin{pmatrix} j_c \\ j_g \end{pmatrix}, \quad (11.53)$$

where

$$\begin{bmatrix} \frac{\partial u^{\text{inc}}}{\partial \xi} & \frac{\partial u^{\text{inc}}}{\partial \eta} \\ \frac{\partial v^{\text{inc}}}{\partial \xi} & \frac{\partial v^{\text{inc}}}{\partial \eta} \end{bmatrix} = -2 \begin{bmatrix} q_1 \xi & q_3 \eta \\ q_2 \xi & q_4 \eta \end{bmatrix}.$$

The deformation gradient, $\mathbf{F} = \mathbf{I} + \nabla \mathbf{u}$, is the sum of the compatible deformation gradient \mathbf{F}_g^c and the incompatible displacement gradient

$$\mathbf{F}_g = \mathbf{F}_g^c + \nabla \mathbf{u}_g^{\text{inc}}. \quad (11.54)$$

Recall that in the back-rotated \mathbf{C}_* of eq. (10.72) and $(\mathbf{Q}_0^T \mathbf{F})_*$ of eq. (10.73), we use the product $\bar{\mathbf{F}} \doteq \mathbf{F} \mathbf{R}_0$ of eq. (10.74), which is now calculated as follows:

$$\bar{\mathbf{F}}_g \doteq \mathbf{F}_g \mathbf{R}_{0g} = \mathbf{F}_g^c \mathbf{R}_{0g} + \nabla \mathbf{u}_g^{\text{inc}} \mathbf{R}_{0g}. \quad (11.55)$$

In the above equation, we still use \mathbf{R}_{0g} at the Gauss point because, as we have verified, if it is replaced by \mathbf{R}_{0c} for the element's center, then the patch test is not satisfied. The compatible term $\mathbf{F}_g^c \mathbf{R}_{0k}$ can be transformed as shown in eq. (10.74).

The functional F_{PE} depends on two sets of variables: the nodal displacements \mathbf{u}_I and the elemental multipliers of incompatible modes \mathbf{q} . The obtained set of FE equations is given by eq. (11.27) and to update the stress and strain multipliers, the scheme U2 of eq. (11.34) should be used.

The finite element for the incompatible displacement gradient of eq. (11.53) is designated as ID4. It is invariant, has a correct rank, and passes

the patch test. Its accuracy and robustness is much better than that of the Q4 element; in linear tests it performs identically as the EAS4 and EADG4 elements.

Note that we can also use only two modes, q_2 and q_3 , and enhance only the shear strain, see eq. (11.39). Such an element (designated as ID2) is particularly useful for shells, for which it performs in a very stable way in nonlinear tests.

11.4.2 EAS4 element

Introduction. The Enhanced Assumed Strain (EAS) method was introduced in [216] and it embodies the following modifications of the ID method:

1. Not displacements but strains are enhanced. The enhancing modes are directly introduced on the level of strains without resorting to displacements.
2. The HW functional is used instead of the PE functional. This change strengthens the variational background and shows the importance of orthogonality of the assumed strain to stress. The crucial result pertaining to the ID method, see eq. (11.47), is fully adopted.

Within the EAS method, the strain for the compatible displacements $\mathbf{E}^c \doteq \mathbf{E}(\mathbf{u}^c)$ is enhanced additively by the strain $\boldsymbol{\varepsilon}^{\text{enh}}$ as follows

$$\underbrace{\boldsymbol{\varepsilon}(\xi, \eta)}_{\text{enhanced}} \doteq \underbrace{\mathbf{E}^c(\xi, \eta)}_{\text{compatible}} + \underbrace{\boldsymbol{\varepsilon}^{\text{enh}}(\xi, \eta)}_{\text{enhancing}}. \quad (11.56)$$

Variational basis of the EAS method. We take the three-field HW functional of eq. (11.1), and use eq. (11.56), which yields

$$F(\mathbf{u}, \boldsymbol{\sigma}, \boldsymbol{\varepsilon}^{\text{enh}}) = \int_B \left[\mathcal{W}(\mathbf{E}^c + \boldsymbol{\varepsilon}^{\text{enh}}) - \boldsymbol{\sigma} \cdot \boldsymbol{\varepsilon}^{\text{enh}} \right] dV - F_{\text{ext}}. \quad (11.57)$$

We wish to eliminate the stress $\boldsymbol{\sigma}$ from this functional, thus we require the enhancing strain to be orthogonal to the stress, i.e.

$$\int_B \boldsymbol{\sigma} \cdot \boldsymbol{\varepsilon}^{\text{enh}} dV = 0, \quad (11.58)$$

for which the term with $\boldsymbol{\sigma}$ in eq. (11.57) vanishes and F becomes the two-field potential energy functional of eq. (11.8) in the following form:

$$F_{\text{PE}}(\mathbf{u}, \boldsymbol{\varepsilon}^{\text{enh}}) = \int_B \mathcal{W}(\mathbf{E}^c + \boldsymbol{\varepsilon}^{\text{enh}}) \, dV - F_{\text{ext}}. \quad (11.59)$$

We note that the orthogonality condition plays an important role in the above derivation, because (1) it allows us to reduce the number of independent fields, (2) it establishes the relation with the elements explicitly using the assumed stress, and (3) it defines the admissible strain enhancements, as such for which the integral (11.58) vanishes for the assumed stress.

Kinematically linear problems. For small strains, i.e. when $\boldsymbol{\varepsilon}_v^c$ is a linear function of \mathbf{u}^c , we proceed as follows. A quadratic Taylor's expansion of the strain energy at some $\boldsymbol{\varepsilon}_v = \boldsymbol{\varepsilon}_v^+$ is as follows

$$\mathcal{W}(\boldsymbol{\varepsilon}_v) \approx \mathcal{W}^+ + \boldsymbol{\sigma}_v^+ \cdot \Delta \boldsymbol{\varepsilon}_v + \frac{1}{2} \Delta \boldsymbol{\varepsilon}_v^T \mathbb{C}^+ \Delta \boldsymbol{\varepsilon}_v, \quad (11.60)$$

where the symbols with “+” are evaluated at $\boldsymbol{\varepsilon}_v^+$, and $(\cdot)_v$ denotes a vector of tensorial components. Besides, $\boldsymbol{\sigma}_v \doteq \partial \mathcal{W} / \partial \boldsymbol{\varepsilon}_v$ is the stress and $\mathbb{C}_{vv} \doteq \partial^2 \mathcal{W} / \partial \boldsymbol{\varepsilon}_v^2$ is the constitutive matrix. For kinematically linear problems, we have $\boldsymbol{\varepsilon}_v^+ = \mathbf{0}$, $\mathcal{W}^+ = 0$, $\boldsymbol{\sigma}_v^+ = \mathbf{0}$, $\Delta \boldsymbol{\varepsilon}_v = \boldsymbol{\varepsilon}_v$, for which we obtain $\mathcal{W}(\boldsymbol{\varepsilon}_v) = \frac{1}{2} \boldsymbol{\varepsilon}_v \cdot (\mathbb{C}_{vv} \boldsymbol{\varepsilon}_v)$. Hence, the strain energy of eq. (11.59) becomes

$$\mathcal{W}(\boldsymbol{\varepsilon}_v^c + \boldsymbol{\varepsilon}_v^{\text{enh}}) = \frac{1}{2} (\boldsymbol{\varepsilon}_v^c + \boldsymbol{\varepsilon}_v^{\text{enh}})^T \mathbb{C}_{vv} (\boldsymbol{\varepsilon}_v^c + \boldsymbol{\varepsilon}_v^{\text{enh}}), \quad (11.61)$$

which can be compared with eq. (11.43) for the ID method. We see that $\boldsymbol{\varepsilon}_v^{\text{enh}}$ plays an analogous role as $\boldsymbol{\varepsilon}_v^{\text{inc}}$ in the ID method.

Enhancing strain. The enhancing strain is constructed as follows:

$$\boldsymbol{\varepsilon}^{\text{enh}} = \mathbf{J}_c^{-T} \boldsymbol{\varepsilon}_\xi \mathbf{J}_c^{-1}, \quad (11.62)$$

which is the transformation rule for covariant components $\boldsymbol{\varepsilon}_\xi$ of a second-rank tensor, from the natural basis at the element's center $\{\mathbf{g}_k^c\}$ to the reference Cartesian basis. We note that the modification of [234], where the Jacobian matrix at the element's center is used to enable passing the patch test by the ID element, is naturally present in eq. (11.62), as a consequence of the use of the basis at element's center. At the Gauss integration point g , we write

$$\boldsymbol{\varepsilon}_g^{\text{enh}} = \mathbf{J}_c^{-T} \boldsymbol{\varepsilon}_{\xi g} \mathbf{J}_c^{-1} \begin{pmatrix} j_c \\ j_g \end{pmatrix}, \quad \boldsymbol{\varepsilon}_\xi \doteq \begin{bmatrix} q_1 \xi & q_3 \xi + q_4 \eta \\ q_3 \xi + q_4 \eta & q_2 \eta \end{bmatrix}, \quad (11.63)$$

where $\boldsymbol{\varepsilon}_\xi$ is a matrix of the assumed strain, and $j \doteq \det \mathbf{J}$. Note that (j_c/j_g) is added, and that the 2×2 -point Gauss integration of it yields $4j_c$, which is the result of the 1-point integration of j . This modification can be compared with that of eq. (11.50) for \mathbf{J}_c^{-1} . The matrix $\boldsymbol{\varepsilon}_\xi$ involves four parameters q_i , and two modes $\{\xi, \eta\}$.

The discrete F_{PE} functional depends on two sets of variables: the nodal displacements \mathbf{u}_I and the elemental multipliers \mathbf{q} of the assumed strain modes. The obtained set of FE equations is given by eq. (11.27) and to update the stress multipliers, the scheme U2 of eq. (11.34) should be used.

The finite element for the assumed strains of eq. (11.62) is designated as EAS4 and, currently, it is a standard in the class of four-node EAS elements. It is invariant, has the correct rank, and passes the patch test. Its accuracy and robustness is much better than that of the Q4 element.

Remark 1. Other representations. Several other forms of $\boldsymbol{\varepsilon}_\xi$ were tested in the literature. The representation with seven parameters (EAS7), obtained from EAS4 by adding the bilinear term $\xi\eta$ to each component, also gained some popularity, but it turned out that it does not satisfy the compatibility condition. The same is true about the five-parameter representation (EAS5), obtained from EAS4 by adding the bilinear term $\xi\eta$ to the shear component only. The EAS2 representation, which uses two parameters for the shear strain enhancement, is particularly stable in non-linear shell applications, but the response is slightly stiffer, which renders that more elements must be used.

Remark 2. Enhancement of Cauchy–Green tensor. In eq. (11.15), the deformation gradient for compatible displacements is written down as $\mathbf{F}^c = \mathbf{F}_\xi \mathbf{J}^{-1}$, for which the Cauchy–Green tensor becomes $\mathbf{C}^c \doteq (\mathbf{F}^c)^T \mathbf{F}^c = \mathbf{J}^{-T} (\mathbf{F}_\xi^T \mathbf{F}_\xi) \mathbf{J}^{-1}$ and involves the transformation $\mathbf{J}^{-T}(\cdot)\mathbf{J}^{-1}$. The same transformation, but with \mathbf{J} replaced by \mathbf{J}_c , is used in eq. (11.62). Hence, when we use the Green strain, we can interpret the EAS method as the enhancement of the Cauchy–Green tensor.

Analytical verification of orthogonality condition for constant stress. Assume that the stress $\boldsymbol{\sigma}$ is constant over the element domain. Then, in eq. (11.64), $\int_B \boldsymbol{\sigma} \cdot \boldsymbol{\varepsilon}^{\text{enh}} dV = \boldsymbol{\sigma} \cdot \int_B \boldsymbol{\varepsilon}^{\text{enh}} dV$, and the orthogonality condition is reduced to

$$\int_B \boldsymbol{\varepsilon}^{\text{enh}} dV = 0, \quad (11.64)$$

which is analogous to eq. (11.47) for the ID method and suffices to pass the patch test. On use of the 2×2 -point Gauss integration, the integral of the enhancing strain becomes

$$\int_B \boldsymbol{\varepsilon}^{\text{enh}} dV = \sum_{g=1}^4 \mathbf{J}_c^{-T} \boldsymbol{\varepsilon}_{\xi g} \mathbf{J}_c^{-1} \begin{pmatrix} j_c \\ j_g \end{pmatrix} j_g = \mathbf{J}_c^{-T} \left(\sum_{g=1}^4 \boldsymbol{\varepsilon}_{\xi g} \right) \mathbf{J}_c^{-1} j_c, \quad (11.65)$$

where eq. (11.62) was used and g is a Gauss point. To satisfy eq. (11.64), it suffices that

$$\sum_{g=1}^4 \boldsymbol{\varepsilon}_{\xi g} = \mathbf{0}. \quad (11.66)$$

We can check that this condition is satisfied for the EAS4 element, because

$$\sum_{g=1}^4 \begin{bmatrix} q_1 \xi_g & q_3 \xi_g + q_4 \eta_g \\ q_3 \xi_g + q_4 \eta_g & q_2 \eta_g \end{bmatrix} = \mathbf{0}, \quad (11.67)$$

for $\xi_g, \eta_g = \pm 1/\sqrt{3}$. This element passes the patch test of Sect. 15.2.3.

Verification of orthogonality condition for non-constant stress. The orthogonality condition is checked for the non-constant five- and seven-parameter stress representations in [256], Appendix B. The stress is assumed as $\boldsymbol{\sigma} = \mathbf{J}_c \boldsymbol{\sigma}^\xi \mathbf{J}_c^T$, which is the transformation rule of the contra-variant tensor components from the $\{\mathbf{g}_k^c\}$ basis at the element center to the reference Cartesian basis. The enhancing strain $\boldsymbol{\varepsilon}^{\text{enh}}$ is taken in the form given by eq. (11.62). Then, the orthogonality condition becomes

$$\int_B \boldsymbol{\sigma} \cdot \boldsymbol{\varepsilon}^{\text{enh}} dV = h \int_{-1}^{+1} \int_{-1}^{+1} \text{tr}[(\mathbf{J}_c \boldsymbol{\sigma}^\xi \mathbf{J}_c^T)^T (\mathbf{J}_c^{-T} \boldsymbol{\varepsilon}_\xi \mathbf{J}_c^{-1})] j d\xi d\eta. \quad (11.68)$$

Evaluating this integral for various forms of $\boldsymbol{\sigma}^\xi$ and $\boldsymbol{\varepsilon}_\xi$, we can test the orthogonality of the involved fields. As $\boldsymbol{\sigma}^\xi$, we take the five-parameter stress of eq. (11.125), or the seven-parameter stress of eq. (12.96), and we use $\boldsymbol{\varepsilon}_\xi$ of eq. (11.62), both assumed either in the natural coordinates $\{\xi, \eta\}$ or in the skew coordinates of eq. (11.81).

We have verified, using a symbolic manipulator, that the orthogonality condition is not satisfied for these representations for irregular elements

but is satisfied for parallelograms. Hence, for irregular elements, the PE functional (11.59) is not fully equivalent to the HW functional (11.57), but only approximates it.

Verification of compatibility of enhancing strains. The compatibility condition for 2D strains is as follows,

$$\frac{\partial^2 \varepsilon_{xx}}{\partial y^2} + \frac{\partial^2 \varepsilon_{yy}}{\partial x^2} = 2 \frac{\partial^2 \varepsilon_{xy}}{\partial x \partial y}. \quad (11.69)$$

It was evaluated for the following specifications of the assumed strain and its derivatives:

1. The enhancing strain in the reference basis is obtained from the assumed representation ε_ξ using eq. (11.62).
2. The first and the second derivatives w.r.t. x, y are expressed by the derivatives w.r.t. ξ, η as specified in eqs. (11.132) and (11.133).

This condition is satisfied in the case of the EAS4 and EAS2 enhancement, only for parallelograms. Because the strain enhancement is added to the compatible strain, eq. (11.56), the total strain has the same property.

The compatibility condition is not satisfied by the EAS5 and EAS7 representations, even for parallelograms, which is caused by the term $\xi\eta$ in ε_{12} . The use of them is therefore not advisable.

Couplings of \mathbf{u}_I and \mathbf{q} in matrix \mathbf{K} . For kinematically nonlinear problems, the tangent matrix \mathbf{K} of eq. (11.28) can be a function of multipliers \mathbf{q} . This is a consequence of couplings of the compatible strain ε^c and the enhancing strain ε^{inc} in the strain energy.

Consider the SVK strain energy, $\mathcal{W}(\varepsilon) \doteq \frac{1}{2}\lambda(\text{tr}\varepsilon)^2 + \mu\text{tr}\varepsilon^2$, where λ and μ are Lamé constants. For $\varepsilon = \varepsilon^c + \varepsilon^{\text{enh}}$, we obtain

$$\begin{aligned} \text{tr}\varepsilon &= \text{tr}\varepsilon^c + \text{tr}\varepsilon^{\text{enh}}, \\ (\text{tr}\varepsilon)^2 &= (\text{tr}\varepsilon^c)^2 + 2(\text{tr}\varepsilon^c)(\text{tr}\varepsilon^{\text{enh}}) + (\text{tr}\varepsilon^{\text{enh}})^2, \\ \varepsilon^2 &= (\varepsilon^c)^2 + (\varepsilon^c\varepsilon^{\text{enh}} + \varepsilon^{\text{enh}}\varepsilon^c) + (\varepsilon^{\text{enh}})^2, \\ \text{tr}(\varepsilon)^2 &= \text{tr}(\varepsilon^c)^2 + 2\text{tr}(\varepsilon^c\varepsilon^{\text{enh}}) + \text{tr}(\varepsilon^{\text{enh}})^2. \end{aligned}$$

Hence, $\mathcal{W}(\varepsilon) \neq \mathcal{W}(\varepsilon^c) + \mathcal{W}(\varepsilon^{\text{enh}})$, i.e. the contribution of ε^c and ε^{enh} to the strain energy is not additive, due to the coupling (underlined) terms. Due to these terms, the tangent matrix $\mathbf{K} \doteq \partial^2\mathcal{W}/\partial\mathbf{u}_I\partial\mathbf{u}_J$ can be a function of multipliers \mathbf{q} and this depends on the type of strain used.

- a) The compatible strain $\boldsymbol{\varepsilon}^c$ is a linear function of \mathbf{u}_I for (i) a kinematically linear problem when $\boldsymbol{\varepsilon} \doteq \frac{1}{2}(\nabla\mathbf{u} + \nabla^T\mathbf{u})$ and (ii) for a nonlinear problem when we use the right stretch strain $\mathbf{H} \doteq \text{sym}[\mathbf{Q}^T(\mathbf{I} + \nabla\mathbf{u})]$. Then the coupling terms do not affect \mathbf{K} .
- b) The compatible strain $\boldsymbol{\varepsilon}^c$ is a quadratic function of \mathbf{u}_I for the Green strain $\mathbf{E} \doteq \frac{1}{2}(\nabla\mathbf{u} + \nabla^T\mathbf{u} + \nabla^T\mathbf{u}\nabla\mathbf{u})$. Then \mathbf{K} for the coupling terms is non-zero and depends on \mathbf{q} .

Summarizing, we obtain additional couplings of \mathbf{u}_I and \mathbf{q} in matrix \mathbf{K} for the Green strain but neither for the infinitesimal strain nor for the right stretch strain.

11.4.3 EADG4 element

The method of Enhanced Assumed Displacement Gradient (EADG) was proposed in [208] and, in fact, its basic concept is deeper rooted in the ID method than the concept of the EAS method which was published two years earlier.

Within the EADG method, the gradient of compatible displacements \mathbf{u}^c is additively enhanced by the enhancing matrix $\tilde{\mathbf{H}}$ as follows:

$$\underbrace{\mathbf{F}(\xi, \eta)}_{\text{enhanced}} \doteq \mathbf{I} + \underbrace{\nabla\mathbf{u}^c(\xi, \eta)}_{\text{compatible}} + \underbrace{\tilde{\mathbf{H}}(\xi, \eta)}_{\text{enhancing}}. \quad (11.70)$$

Construction of $\tilde{\mathbf{H}}$. In eq. (11.53) for the ID method, the incompatible displacements were differentiated to calculate the matrix

$$\begin{bmatrix} \frac{\partial u^{\text{inc}}}{\partial \xi} & \frac{\partial u^{\text{inc}}}{\partial \eta} \\ \frac{\partial v^{\text{inc}}}{\partial \xi} & \frac{\partial v^{\text{inc}}}{\partial \eta} \end{bmatrix} = -2 \begin{bmatrix} q_1\xi & q_3\eta \\ q_2\xi & q_4\eta \end{bmatrix}.$$

In the EADG method, we directly assume the form of this matrix, designated as \mathbf{G}^ξ , without resorting to the concept of incompatible displacements and without differentiation. Equation (11.53) of the ID method is rewritten for the EADG method as follows:

$$\tilde{\mathbf{H}}_g \doteq \mathbf{J}_c \mathbf{G}_g^\xi \mathbf{J}_c^{-1} \begin{pmatrix} j_c \\ j_g \end{pmatrix}, \quad \mathbf{G}^\xi \doteq \begin{bmatrix} q_1\xi & q_3\eta \\ q_2\xi & q_4\eta \end{bmatrix}, \quad (11.71)$$

where the factor (-2) was omitted in \mathbf{G}^ξ and g is a Gauss point. Other representations can also be used in \mathbf{G}^ξ so the EADG and EAS methods are equally versatile.

Variational basis of the EADG method. The EADG method is based on the three-field HW functional, although involving not strains but the deformation gradient

$$F(\mathbf{u}, \mathbf{F}, \mathbf{P}) \doteq \int_B \{ \mathcal{W}(\mathbf{F}^T \mathbf{F}) + \mathbf{P} \cdot [(\mathbf{I} + \nabla \mathbf{u}) - \mathbf{F}] \} dV - F_{\text{ext}}, \quad (11.72)$$

where \mathbf{P} is the nominal stress, \mathbf{F} is an independent field, and F_{ext} is a potential of the body force, the external loads, and the displacement boundary conditions. Note that \mathbf{P} serves as a Lagrange multiplier for the relation $(\mathbf{I} + \nabla \mathbf{u}) - \mathbf{F}$.

Using eq. (11.70), we obtain

$$F(\mathbf{u}, \tilde{\mathbf{H}}, \mathbf{P}) = \int_B \{ \mathcal{W}[(\mathbf{I} + \nabla \mathbf{u} + \tilde{\mathbf{H}})^T (\mathbf{I} + \nabla \mathbf{u} + \tilde{\mathbf{H}})] - \mathbf{P} \cdot \tilde{\mathbf{H}} \} dV - F_{\text{ext}}, \quad (11.73)$$

in which we do not have \mathbf{F} but the enhancing $\tilde{\mathbf{H}}$. If the assumed $\tilde{\mathbf{H}}$ is orthogonal to the stress, i.e. $\int_B \mathbf{P} \cdot \tilde{\mathbf{H}} dV = 0$, then the last term of the above functional vanishes and we obtain a two-field enhanced PE functional

$$F_{\text{PE}}(\mathbf{u}, \tilde{\mathbf{H}}) = \int_B \mathcal{W}[(\mathbf{I} + \nabla \mathbf{u} + \tilde{\mathbf{H}})^T (\mathbf{I} + \nabla \mathbf{u} + \tilde{\mathbf{H}})] dV - F_{\text{ext}}, \quad (11.74)$$

which does not depend on the stress \mathbf{P} .

The discrete F_{PE} functional depends on two types of variables: the nodal displacements \mathbf{u}_I and the elemental multipliers \mathbf{q} of assumed displacement gradient modes. The obtained set of FE equations is given by eq. (11.27), and the scheme U2 of eq. (11.34) should be used to update the stress multipliers.

The finite element for the representation of eq. (11.71) is designated as EADG4 and, currently, it is a standard in the class of four-node EADG elements. It is invariant, has a correct rank, and passes the patch test. Its accuracy and robustness are much better than those of the Q4 element. In linear tests, it performs identically as ID4 and EAS4 elements, but is superior to them in the case of elements with a drilling rotation, see Sect. 12.

Remark 1. Relation to EAS method. The EADG and ID method use the $\mathbf{J}_c(\cdot) \mathbf{J}_c^{-1}$ transformation, see eqs. (11.53) and (11.71), while the EAS method is based on the $\mathbf{J}_c^{-T}(\cdot) \mathbf{J}_c^{-1}$ transformation, see eq. (11.62).

These transformations are identical only when $\mathbf{J}_c = \mathbf{J}_c^{-T}$, e.g. when $\mathbf{J}_c \in \text{SO}(3)$. Hence, in general, these methods are different although based on the same concept and perform similarly in some tests. The variational foundations of the assumed strain methods are revised in [215].

Remark 2. Spatial formulation. Using the deformation function, $\chi : \mathbf{x} = \chi(\mathbf{y})$, the approximation of eq. (11.70) can be rewritten as $\mathbf{F} = \nabla\chi + \tilde{\mathbf{H}}$. Defining the spatial enhanced displacement gradient $\tilde{\mathbf{h}} \doteq \tilde{\mathbf{H}}\nabla\chi^{-1}$, we obtain $\mathbf{F} = (\mathbf{I} + \tilde{\mathbf{h}})\nabla\chi$, in which the enhanced deformation gradient $(\mathbf{I} + \tilde{\mathbf{h}})$ is superposed multiplicatively on the standard deformation gradient $\nabla\chi$. This form of \mathbf{F} and the variational problem in the spatial setting, i.e. $\mathbf{P} \cdot \delta\mathbf{F} = \boldsymbol{\tau} \cdot [\nabla(\delta\mathbf{u})\mathbf{F}^{-1}]$, where $\boldsymbol{\tau}$ is the Kirchhoff stress, are used in [208].

Finally, we note that some enhanced strain elements can experience problems in the range of large compressive strains. This problem was detected in [63] and studied in [264], where a single square element was compressed by two equal forces and the solution was obtained for the compressible neo-Hookean material. At the first zero eigenvalue, the non-symmetric bifurcation point was obtained. This test can also be performed for a block of elements, as in [263] where the eigenvector at the bifurcation point is checked for the presence of hourglassing. This topic is also addressed in [154].

11.5 Mixed Hellinger–Reissner and Hu–Washizu elements

Definition of mixed formulations. To improve the performance of early elements, several non-standard formulations were tested, including the mixed formulation in [168], and the hybrid mixed formulation in [121]. A lot of work has been done since these pioneering papers to improve mixed methods; the elements and their theoretical foundations.

Various definitions exist of the *mixed* formulation in the literature; we adopt the one referring to the features of the governing functional:

1. the governing functional must depend on several types of variables,
2. some of the variables must be Lagrange multipliers. Hence, the governing functional attains a saddle point, not a minimum, at a solution.

This definition implies that the Hellinger–Reissner (HR) functional and the Hu–Washizu (HW) functional are mixed, but the potential energy

(PE) functional is not. For shells, the formulations with rotations of Sect. 4 are mixed but the use of the Reissner hypothesis does not yield a mixed formulation, although it introduces the rotational dofs. Note that the formulation remains mixed, even if the multipliers are eliminated by a local regularization of the functional.

Compared with the standard elements, the mixed elements have the following features:

1. the inter-element continuity of certain fields is relaxed,
2. the level of non-linearity for finite strains is reduced,
3. the non-zero eigenvalues of the non-reduced tangent matrix of eq. (11.27) for mixed elements are either positive or negative because the discrete HR and HW functionals have a saddle point at $(\mathbf{u} = \mathbf{0}, \mathbf{q} = \mathbf{0})$. The number of negative eigenvalues is identical to the number of stress parameters, i.e. five in Fig. 11.4.

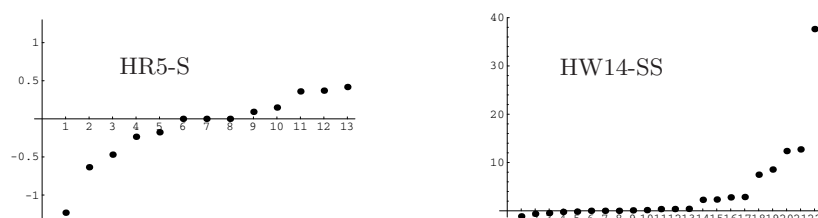


Fig. 11.4 Eigenvalues of non-reduced matrix of mixed elements.

The mixed finite elements show (i) a slightly higher accuracy of displacements and stresses for coarse distorted meshes, (ii) a better convergence rate in non-linear problems than elements based on other formulations. They can be cast in a similar form to the standard elements by eliminating the additional variables on the element level.

In this section, we describe 2D mixed elements based on the HR and the HW functionals. We also provide comments on the mixed/enhanced elements.

Skew coordinates. To define the representation of stress (and strain) in mixed elements, we use the skew coordinates instead of the natural coordinates as proposed in [256, 257]. This modification improves the accuracy of mixed elements.

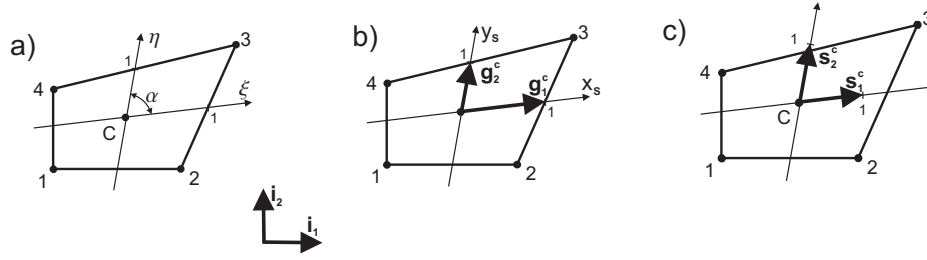


Fig. 11.5 Bases at element's center. a) Natural coordinates $\{\xi, \eta\}$. b) Natural basis $\{\mathbf{g}_k^c\}$ and skew coordinates $\{x_S, y_S\}$. c) Oblique basis $\{\mathbf{s}_k^c\}$, which is not used here!

The skew coordinates relative to the natural basis at the element's center $\{\mathbf{g}_k^c\}$ are designated by $\{x_S, y_S\}$. They can be defined in relation to the Cartesian coordinates $\{x, y\}$ associated with the reference basis $\{\mathbf{i}_k\}$ as follows:

The position vector of a particle in the initial configuration can be expressed in the reference Cartesian basis, see Fig. 11.5A, as $\mathbf{y} = x\mathbf{i}_1 + y\mathbf{i}_2$, where x, y are approximated by the bilinear shape functions of ξ, η of eq. (11.10). Consider the position vector relative to the element's center, i.e. $\bar{\mathbf{y}} = \mathbf{y} - \mathbf{y}_c$, and write it relative to these two bases as follows

$$\bar{\mathbf{y}} = \bar{x}\mathbf{i}_1 + \bar{y}\mathbf{i}_2 = x_S\mathbf{g}_1^c + y_S\mathbf{g}_2^c. \quad (11.75)$$

Taking the scalar product of this equation with the vectors \mathbf{i}_1 and \mathbf{i}_2 , we obtain two equations which can be written in the following form:

$$\begin{bmatrix} \bar{x} \\ \bar{y} \end{bmatrix} = \mathbf{J}_c \begin{bmatrix} x_S \\ y_S \end{bmatrix}, \quad \mathbf{J}_c = \begin{bmatrix} \mathbf{g}_1^c \cdot \mathbf{i}_1 & \mathbf{g}_2^c \cdot \mathbf{i}_1 \\ \mathbf{g}_1^c \cdot \mathbf{i}_2 & \mathbf{g}_2^c \cdot \mathbf{i}_2 \end{bmatrix}, \quad (11.76)$$

where \mathbf{J}_c is the Jacobian of eq. (11.13) at the element's center. Then the skew coordinates are calculated as

$$\begin{bmatrix} x_S \\ y_S \end{bmatrix} = \mathbf{J}_c^{-1} \begin{bmatrix} \bar{x} \\ \bar{y} \end{bmatrix}. \quad (11.77)$$

This relation implies

$$\mathbf{J}_c^{-1} = \begin{bmatrix} \frac{\partial x_S}{\partial \bar{x}} & \frac{\partial x_S}{\partial \bar{y}} \\ \frac{\partial y_S}{\partial \bar{x}} & \frac{\partial y_S}{\partial \bar{y}} \end{bmatrix}. \quad (11.78)$$

For the position vector of eq. (11.10) rewritten as

$$\begin{bmatrix} x \\ y \end{bmatrix} = \begin{bmatrix} a_0 + a_1\xi + a_2\eta + a_3\xi\eta \\ b_0 + b_1\xi + b_2\eta + b_3\xi\eta \end{bmatrix}, \quad (11.79)$$

where the coefficients a_i, b_i are functions of the positions of nodes, we have

$$\begin{bmatrix} \bar{x} \\ \bar{y} \end{bmatrix} \doteq \begin{bmatrix} x - a_0 \\ y - b_0 \end{bmatrix} = \begin{bmatrix} a_1\xi + a_2\eta + a_3\xi\eta \\ b_1\xi + b_2\eta + b_3\xi\eta \end{bmatrix}, \quad (11.80)$$

where a_0, b_0 are coordinates of the element's center. Using this relation in eq. (11.77), the skew coordinates become the following functions of the natural coordinates:

$$\begin{bmatrix} x_S \\ y_S \end{bmatrix} = \begin{bmatrix} \xi + A\xi\eta \\ \eta + B\xi\eta \end{bmatrix}, \quad (11.81)$$

where

$$A \doteq \frac{a_3b_2 - a_2b_3}{a_1b_2 - a_2b_1}, \quad B \doteq \frac{a_1b_3 - a_3b_1}{a_1b_2 - a_2b_1}.$$

The coefficients A and B can be expressed using the determinant of the Jacobian \mathbf{J} of eq. (11.13). This Jacobian, using eq. (11.79), becomes

$$\mathbf{J} \doteq \begin{bmatrix} \mathbf{g}_1 \cdot \mathbf{i}_1 & \mathbf{g}_2 \cdot \mathbf{i}_1 \\ \mathbf{g}_1 \cdot \mathbf{i}_2 & \mathbf{g}_2 \cdot \mathbf{i}_2 \end{bmatrix} = \begin{bmatrix} a_1 + a_3\eta & a_2 + a_3\xi \\ b_1 + b_3\eta & b_2 + b_3\xi \end{bmatrix}, \quad (11.82)$$

where $\mathbf{g}_1, \mathbf{g}_2$ are defined in eq. (11.11). Note that this Jacobian is not associated with the element's center, differently from the Jacobian of eq. (11.76). We can expand the determinant of this Jacobian as follows:

$$\det \mathbf{J} = j_c + (j, \xi)_c \xi + (j, \eta)_c \eta, \quad (11.83)$$

where $j_c = a_1b_2 - a_2b_1$, $(j, \xi)_c = a_1b_3 - a_3b_1$, and $(j, \eta)_c = a_3b_2 - a_2b_3$. Hence, an alternative form of the coefficients is

$$A = \frac{(j, \eta)_c}{j_c}, \quad B = \frac{(j, \xi)_c}{j_c}. \quad (11.84)$$

For the elements of a parallelogram shape, $(j, \xi)_c = (j, \eta)_c = 0$, so $A = B = 0$ and, by eq. (11.81), the skew coordinates $\{x_S, y_S\}$ are equal to the natural coordinates $\{\xi, \eta\}$.

Remark 1. It is a common error that the natural coordinates are treated as being associated with the natural basis at the element's center. To prove that it is incorrect, it suffices to define the position vector not as $\bar{\mathbf{y}} = x_S \mathbf{g}_1^c + y_S \mathbf{g}_2^c$, which is the correct form, but using the natural coordinates,

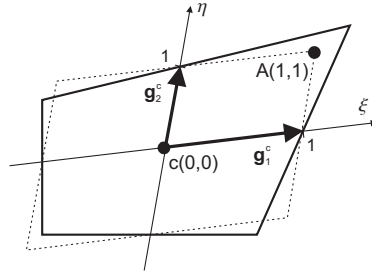


Fig. 11.6 “Fictitious” parallelogram yielded by the use of natural coordinates.

i.e. as $\bar{\mathbf{y}} = \xi \mathbf{g}_1^c + \eta \mathbf{g}_2^c$. For the latter form and $\xi, \eta \in [-1, +1]$, we obtain a “fictitious” parallelogram element as shown in Fig. 11.6 by the dotted line. The difference between the two forms of $\bar{\mathbf{y}}$ vanishes for parallelograms, as then the skew and natural coordinates are identical.

Remark 2. In literature, the idea to replace a trapezoidal element by an “equivalent” parallelogram element, identical with the “fictitious” parallelogram of Fig. 11.6, is put forward. Note, however, that the “equivalent” element does not pass the patch test!

Remark 3. Note that we can also define another basis at the element’s center, the so-called oblique basis, as follows:

$$\mathbf{s}_1^c \doteq \frac{\mathbf{g}_1^c}{\|\mathbf{g}_1^c\|}, \quad \mathbf{s}_2^c \doteq \frac{\mathbf{g}_2^c}{\|\mathbf{g}_2^c\|}, \quad (11.85)$$

where \mathbf{s}_k^c are unit vectors, co-linear with the natural basis, see Fig. 11.5C. The oblique basis and the corresponding oblique coordinates are described in [151] where they are used to skew membranes and plates. They were also applied in several elements, e.g., in [184]. The advantage of using the oblique stresses is that the bi-harmonic equation retains a simple form. Therefore, the Airy stress function can be easily found and the homogeneous equilibrium equation and the strain compatibility equation are satisfied. The disadvantage is that the oblique stresses are different from the real stresses, for which the constitutive equation is written, see [151], p. 25. The oblique basis and the associated coordinates are not used in our work.

Inf-sup (LBB) condition. In mixed formulations, the full (non-reduced) tangent matrix of eq. (11.27) is not positive definite, which can cause problems with the well-posedness of the equations, i.e. with solvability and stability. The requirement to safely solve the system of equations is called the *inf-sup* condition and there is a vast mathematical literature related to it, see e.g. [11, 12, 38, 37, 193]. This condition depends on the FE discretization and, hence, analytical expressions are difficult and beyond the scope of this work.

On the other hand, we can much easier check a numerical counterpart of this condition, called the LBB condition, where the LBB is the acronym for the names Ladyzhenskaya–Babuška–Brezzi. Below, we consider the problem which is kinematically and materially linear, using a procedure similar to that presented in [38].

For the purely displacement formulation, the FE equilibrium equations have the form

$$\mathbf{K}_0 \mathbf{u} = \mathbf{p}, \quad (11.86)$$

where \mathbf{K}_0 is the tangent matrix, \mathbf{u} is the vector of nodal values of displacements, and \mathbf{p} is the vector of external nodal loads. Equation (11.86) is well-posed if the following condition of positive definiteness (ellipticity) is satisfied

$$\exists \beta > 0 \quad \mathbf{u}^T \mathbf{K}_0 \mathbf{u} \geq \beta \|\mathbf{u}\|^2 \quad (11.87)$$

for an arbitrary non-zero vector \mathbf{u} and some norm $\|\cdot\|$ for the space of \mathbf{u} . Usually, the energy norm is used, i.e. $\|\mathbf{u}\|^2 = \mathbf{u}^T \mathbf{K}_0 \mathbf{u}$, and then $\beta = 1$. Below, we consider the mixed formulations and procedures for obtaining their reduced displacement form.

Inf-sup (LBB) for two-field mixed formulation. For a mixed two-field formulation, the equilibrium equations have the form

$$\begin{bmatrix} \mathbf{0} & \mathbf{L} \\ \mathbf{L}^T & \mathbf{K} \end{bmatrix} \begin{bmatrix} \mathbf{u} \\ \mathbf{q} \end{bmatrix} = \begin{bmatrix} \mathbf{p} \\ \mathbf{0} \end{bmatrix}, \quad (11.88)$$

where \mathbf{q} is the vector of additional variables, e.g. the stress parameters for the HR functional. The matrix of eq. (11.88) is symmetric, but indefinite i.e. has positive and negative eigenvalues. The sub-matrix \mathbf{K} is symmetric and positive definite, \mathbf{L} can be rectangular.

To obtain the reduced displacement form of the mixed equations, we calculate $\mathbf{q} = \mathbf{K}^{-1} \mathbf{L}^T \mathbf{u}$ from the second equation of the system (11.88) and use it in the first equation,

$$\mathbf{K}^* \mathbf{u} = \mathbf{p}, \quad \text{where } \mathbf{K}^* \doteq \mathbf{L} \mathbf{K}^{-1} \mathbf{L}^T. \quad (11.89)$$

This equation is well-posed if

$$\exists \beta > 0 \quad \mathbf{u}^T \mathbf{K}^* \mathbf{u} \geq \beta \|\mathbf{u}\|^2, \quad (11.90)$$

for an arbitrary non-zero vector \mathbf{u} . We can use the energy norm, $\|\mathbf{u}\|^2 \doteq \mathbf{u}^T \mathbf{K}_0 \mathbf{u}$, where \mathbf{K}_0 is the matrix of the purely displacement eq. (11.86), so the above condition becomes

$$\exists \beta > 0 \quad \mathbf{u}^T \mathbf{K}^* \mathbf{u} \geq \beta \mathbf{u}^T \mathbf{K}_0 \mathbf{u}. \quad (11.91)$$

Thus, we have to find

$$\beta \doteq \inf_{\mathbf{u}} \frac{\mathbf{u}^T \mathbf{K}^* \mathbf{u}}{\mathbf{u}^T \mathbf{K}_0 \mathbf{u}} \quad (11.92)$$

and check whether $\beta > 0$. The fraction on the r.h.s. is the Rayleigh quotient, hence β is the smallest eigenvalue of the generalized eigenvalue problem

$$\mathbf{K}^* \mathbf{u} = \gamma \mathbf{K}_0 \mathbf{u}. \quad (11.93)$$

A more general form of eq. (11.92) is obtained if we note that $\mathbf{u}^T \mathbf{K}^* \mathbf{u} = \mathbf{u}^T \mathbf{L} \mathbf{K}^{-1} \mathbf{L}^T \mathbf{u}$ and use the following *equivalence*:

$$\mathbf{u}^T \mathbf{L} \mathbf{K}^{-1} \mathbf{L}^T \mathbf{u} = \sup_{\mathbf{q}} \frac{(\mathbf{q}^T \mathbf{L}^T \mathbf{u})^2}{\mathbf{q}^T \mathbf{K} \mathbf{q}}, \quad (11.94)$$

the proof of which is given below. Then we obtain the *inf-sup* condition for the system (11.88),

$$\beta \doteq \inf_{\mathbf{u}} \sup_{\mathbf{q}} \frac{(\mathbf{q}^T \mathbf{L}^T \mathbf{u})^2}{(\mathbf{q}^T \mathbf{K} \mathbf{q}) (\mathbf{u}^T \mathbf{K}_0 \mathbf{u})} > 0. \quad (11.95)$$

The advantage of this condition is that it does not contain inverse matrices, i.e. we don't have to solve the problem to see if it is solvable.

Proof of equivalence, eq. (11.94). ([12], Sect. 7) The crucial fact is that \mathbf{K} is symmetric and positive definite, so there exists a symmetric and positive definite $\mathbf{K}^{1/2}$ such that $\mathbf{K}^{1/2} \mathbf{K}^{1/2} = \mathbf{K}$. Let us denote $\mathbf{w} \doteq \mathbf{K}^{1/2} \mathbf{q}$, so $\mathbf{q} \doteq \mathbf{K}^{-1/2} \mathbf{w}$. By substituting \mathbf{q}^T , we have

$$\sup_{\mathbf{q}} \frac{(\mathbf{q}^T \mathbf{L}^T \mathbf{u})^2}{\mathbf{q}^T \mathbf{K} \mathbf{q}} = \sup_{\mathbf{w}} \frac{(\mathbf{w}^T \mathbf{K}^{-1/2} \mathbf{L}^T \mathbf{u})^2}{\mathbf{w}^T \mathbf{w}} \quad (11.96)$$

and we shall prove that

$$\mathbf{u}^T \mathbf{L} \mathbf{K}^{-1} \mathbf{L}^T \mathbf{u} = \sup_{\mathbf{w}} \frac{(\mathbf{w}^T \mathbf{K}^{-1/2} \mathbf{L}^T \mathbf{u})^2}{\mathbf{w}^T \mathbf{w}}, \quad (11.97)$$

instead of eq. (11.94). The proof is divided into two parts.

- (i) The Schwartz inequality, $(\mathbf{a}^T \mathbf{b})^2 \leq (\mathbf{a}^T \mathbf{a})(\mathbf{b}^T \mathbf{b})$, with vectors $\mathbf{a} \doteq \mathbf{w}$ and $\mathbf{b} \doteq \mathbf{K}^{-1/2} \mathbf{L}^T \mathbf{u}$, yields

$$(\mathbf{w}^T \mathbf{K}^{-1/2} \mathbf{L}^T \mathbf{u})^2 \leq (\mathbf{w}^T \mathbf{w})(\mathbf{u}^T \mathbf{L} \mathbf{K}^{-1/2} \mathbf{K}^{-1/2} \mathbf{L}^T \mathbf{u}), \quad (11.98)$$

and dividing both sides by $\mathbf{w}^T \mathbf{w} = \mathbf{q}^T \mathbf{K} \mathbf{q} \neq 0$, we obtain

$$\sup_{\mathbf{w}} \frac{(\mathbf{w}^T \mathbf{K}^{-1/2} \mathbf{L}^T \mathbf{u})^2}{\mathbf{w}^T \mathbf{w}} \leq \mathbf{u}^T \mathbf{L} \mathbf{K}^{-1} \mathbf{L}^T \mathbf{u}. \quad (11.99)$$

- (ii) Selecting $\mathbf{w} = \mathbf{K}^{-1/2} \mathbf{L}^T \mathbf{u}$ and using it in the r.h.s. of eq. (11.97), we obtain

$$\begin{aligned} & \sup_{\mathbf{w}} \frac{(\mathbf{w}^T \mathbf{K}^{-1/2} \mathbf{L}^T \mathbf{u})^2}{\mathbf{w}^T \mathbf{w}} \\ & \geq \frac{(\mathbf{u}^T \mathbf{L} \mathbf{K}^{-1/2} \mathbf{K}^{-1/2} \mathbf{L}^T \mathbf{u})^2}{\mathbf{u}^T \mathbf{L} \mathbf{K}^{-1/2} \mathbf{K}^{-1/2} \mathbf{L}^T \mathbf{u}} = \mathbf{u}^T \mathbf{L} \mathbf{K}^{-1} \mathbf{L}^T \mathbf{u}. \end{aligned} \quad (11.100)$$

The inequalities (11.100) and (11.99) imply eq. (11.97) and, in turn, the *equivalence* of eq. (11.94). \square

Inf-sup (LBB) for three-field mixed formulation. For a mixed three-field formulation, the equilibrium equations have the form

$$\begin{bmatrix} \mathbf{0} & \mathbf{L}_1 & \mathbf{0} \\ \mathbf{L}_1^T & \mathbf{0} & \mathbf{K}_{12} \\ \mathbf{0} & \mathbf{K}_{12}^T & \mathbf{K}_{22} \end{bmatrix} \begin{bmatrix} \mathbf{u} \\ \mathbf{q}_1 \\ \mathbf{q}_2 \end{bmatrix} = \begin{bmatrix} \mathbf{p} \\ \mathbf{0} \\ \mathbf{0} \end{bmatrix}, \quad (11.101)$$

where \mathbf{q}_1 and \mathbf{q}_2 are vectors of additional variables. For instance, for the HW functional, \mathbf{q}_1 is the vector of stress parameters and \mathbf{q}_2 is the vector of strain parameters. The matrix in eq. (11.101) is symmetric but indefinite i.e. has positive and negative eigenvalues. The sub-matrix \mathbf{K}_{22} is symmetric and positive definite, \mathbf{K}_{12} and \mathbf{L}_1 can be rectangular. The above set is solved as a sequence of two problems, each for two fields only.

Problem 1. The first problem is intermediate, i.e. needed to solve *Problem 2*, and is defined by the set of equations

$$\begin{bmatrix} \mathbf{0} & \mathbf{K}_{12} \\ \mathbf{K}_{12}^T & \mathbf{K}_{22} \end{bmatrix} \begin{bmatrix} \mathbf{q}_1 \\ \mathbf{q}_2 \end{bmatrix} = \begin{bmatrix} -\mathbf{L}_1^T \mathbf{u} \\ \mathbf{0} \end{bmatrix}, \quad (11.102)$$

which is analogous to eq. (11.88) for two-field mixed formulation. (Note that for \mathbf{u} , we use the energy norm $\|\mathbf{u}\|^2 \doteq \mathbf{u}^T \mathbf{K}_0 \mathbf{u}$, while for \mathbf{q}_1 , we shall use the Euclidean norm $\|\mathbf{q}_1\|^2 = \mathbf{q}_1^T \mathbf{q}_1$.) To solve this set, first, from the second equation, we calculate $\mathbf{q}_2 = -\mathbf{K}_{22}^{-1} \mathbf{K}_{12}^T \mathbf{q}_1$, which is possible because \mathbf{K}_{22} is invertible. Next we use \mathbf{q}_2 in the first equation to obtain

$$\bar{\mathbf{K}} \mathbf{q}_1 = \mathbf{L}_1 \mathbf{u}, \quad \text{where} \quad \bar{\mathbf{K}} \doteq \mathbf{K}_{12} \mathbf{K}_{22}^{-1} \mathbf{K}_{12}^T. \quad (11.103)$$

This equation is solvable if $\bar{\mathbf{K}}$ is positive definite, i.e.

$$\exists \beta_1 > 0 \quad \mathbf{q}_1^T \bar{\mathbf{K}} \mathbf{q}_1 \geq \beta_1 \|\mathbf{q}_1\|^2, \quad (11.104)$$

or, for the Euclidean norm $\|\mathbf{q}_1\|^2 = \mathbf{q}_1^T \mathbf{q}_1$,

$$\exists \beta_1 > 0 \quad \mathbf{q}_1^T \bar{\mathbf{K}} \mathbf{q}_1 \geq \beta_1 \mathbf{q}_1^T \mathbf{q}_1, \quad (11.105)$$

for any non-zero vector \mathbf{q}_1 . Thus, we have to find

$$\beta_1 \doteq \inf_{\mathbf{q}_1} \frac{\mathbf{q}_1^T \bar{\mathbf{K}} \mathbf{q}_1}{\mathbf{q}_1^T \mathbf{q}_1} \quad (11.106)$$

and check that $\beta_1 > 0$. The fraction on the r.h.s. is the Rayleigh quotient, so β_1 is the smallest eigenvalue of the standard eigenvalue problem

$$\bar{\mathbf{K}} \mathbf{q}_1 = \gamma_1 \mathbf{q}_1, \quad (11.107)$$

which can be used to verify numerically the well-posedness of *Problem 1*. On use of the *equivalence* of eq. (11.94)

$$\mathbf{q}_1^T \bar{\mathbf{K}} \mathbf{q}_1 = \mathbf{q}_1^T \mathbf{K}_{12} \mathbf{K}_{22}^{-1} \mathbf{K}_{12}^T \mathbf{q}_1 = \sup_{\mathbf{q}_2} \frac{(\mathbf{q}_2^T \mathbf{K}_{12}^T \mathbf{q}_1)^2}{\mathbf{q}_2^T \mathbf{K}_{22} \mathbf{q}_2}, \quad (11.108)$$

so the *inf-sup* condition for *Problem 1* is analogous to eq. (11.95),

$$\beta_1 \doteq \inf_{\mathbf{q}_1} \sup_{\mathbf{q}_2} \frac{(\mathbf{q}_2^T \mathbf{K}_{12}^T \mathbf{q}_1)^2}{(\mathbf{q}_2^T \mathbf{K}_{22} \mathbf{q}_2) (\mathbf{q}_1^T \mathbf{q}_1)} > 0. \quad (11.109)$$

This condition does not require calculation of the inverse \mathbf{K}_{22}^{-1} and can be written in an alternative form,

$$\forall \mathbf{q}_1 \exists \mathbf{q}_2 \quad (\mathbf{q}_2^T \mathbf{K}_{12}^T \mathbf{q}_1)^2 > \beta_1 (\mathbf{q}_2^T \mathbf{K}_{22} \mathbf{q}_2)(\mathbf{q}_1^T \mathbf{q}_1) \quad \text{for some } \beta_1 > 0, \quad (11.110)$$

allowing us to deduce that \mathbf{q}_1 cannot belong to the null space of \mathbf{K}_{12}^T , i.e. \mathbf{K}_{12}^T must have the rank equal to the number of columns and that $\mathbf{K}_{12} \mathbf{q}_2$ cannot be orthogonal to the space of \mathbf{q}_1 's.

Problem 2. Using $\mathbf{q}_2 = -\mathbf{K}_{22}^{-1} \mathbf{K}_{12}^T \mathbf{q}_1$ in the second of the full set of equation (11.101), the first two equations form the set

$$\begin{bmatrix} \mathbf{0} & \mathbf{L}_1 \\ \mathbf{L}_1^T & -\bar{\mathbf{K}} \end{bmatrix} \begin{bmatrix} \mathbf{u} \\ \mathbf{q}_1 \end{bmatrix} = \begin{bmatrix} \mathbf{p} \\ \mathbf{0} \end{bmatrix}, \quad (11.111)$$

which is analogous to eq. (11.88) for two-field mixed formulation. The matrix $\bar{\mathbf{K}}$ is symmetric and, if eq. (11.109) is satisfied for *Problem 1*, then it is also positive definite. From the second equation of (11.111), we can calculate: $\mathbf{q}_1 = \bar{\mathbf{K}}^{-1} \mathbf{L}_1^T \mathbf{u}$, and use it in the first equation to obtain the reduced displacement form of the mixed equations

$$\mathbf{K}^* \mathbf{u} = \mathbf{p}, \quad \text{where } \mathbf{K}^* \doteq \mathbf{L}_1 \bar{\mathbf{K}}^{-1} \mathbf{L}_1^T. \quad (11.112)$$

This equation is solvable if \mathbf{K}^* is positive definite, i.e.

$$\exists \beta_2 > 0 \quad \mathbf{u}^T \mathbf{K}^* \mathbf{u} \geq \beta_2 \|\mathbf{u}\|^2, \quad (11.113)$$

for an arbitrary non-zero vector \mathbf{u} . We can use the energy norm $\|\mathbf{u}\|^2 \doteq \mathbf{u}^T \mathbf{K}_0 \mathbf{u}$, where \mathbf{K}_0 is the matrix of the purely displacement eq. (11.86), so the above condition becomes

$$\exists \beta_2 > 0 \quad \mathbf{u}^T \mathbf{K}^* \mathbf{u} \geq \beta_2 \mathbf{u}^T \mathbf{K}_0 \mathbf{u}. \quad (11.114)$$

Thus, we have to find

$$\beta_2 \doteq \inf_{\mathbf{u}} \frac{\mathbf{u}^T \mathbf{K}^* \mathbf{u}}{\mathbf{u}^T \mathbf{K}_0 \mathbf{u}} \quad (11.115)$$

and check whether $\beta_2 > 0$. The fraction on the r.h.s. is the Rayleigh quotient, so β_2 is the smallest eigenvalue of the generalized eigenvalue problem

$$\mathbf{K}^* \mathbf{u} = \gamma_2 \mathbf{K}_0 \mathbf{u}. \quad (11.116)$$

If we write $\mathbf{u}^T \mathbf{K}^* \mathbf{u} = \mathbf{u}^T \mathbf{L}_1 \bar{\mathbf{K}}^{-1} \mathbf{L}_1^T \mathbf{u}$ and use the *equivalence* eq. (11.94), we obtain the *inf-sup* form of eq. (11.115),

$$\beta_2 \doteq \inf_{\mathbf{u}} \sup_{\mathbf{q}_1} \frac{(\mathbf{q}_1^T \mathbf{L}_1^T \mathbf{u})^2}{(\mathbf{q}_1^T \bar{\mathbf{K}} \mathbf{q}_1) (\mathbf{u}^T \mathbf{K}_0 \mathbf{u})} > 0. \quad (11.117)$$

Note that $\bar{\mathbf{K}}$ depends on the inverse \mathbf{K}_{22}^{-1} , which we eliminate as follows. The property $[\sup_{\mathbf{x}} F(\mathbf{x})]^{-1} = \inf_{\mathbf{x}} F^{-1}(\mathbf{x})$ holds for a scalar continuous function $F(\mathbf{x}) > 0$. We take

$$\mathbf{x} \doteq \mathbf{q}_2, \quad F(\mathbf{q}_2) \doteq \frac{(\mathbf{q}_2^T \mathbf{K}_{12}^T \mathbf{q}_1)^2}{\mathbf{q}_2^T \mathbf{K}_{22} \mathbf{q}_2}, \quad (11.118)$$

where $F(\mathbf{q}_2) > 0$ by eq. (11.109). Then the inverse of eq. (11.108) is

$$\frac{1}{\mathbf{q}_1^T \bar{\mathbf{K}} \mathbf{q}_1} = \inf_{\mathbf{q}_2} \frac{\mathbf{q}_2^T \mathbf{K}_{22} \mathbf{q}_2}{(\mathbf{q}_2^T \mathbf{K}_{12}^T \mathbf{q}_1)^2} \quad (11.119)$$

and we use it in eq. (11.117), obtaining the *inf-sup* condition for the three-field mixed problem,

$$\beta_2 \doteq \inf_{\mathbf{u}} \sup_{\mathbf{q}_1} \inf_{\mathbf{q}_2} \frac{(\mathbf{q}_2^T \mathbf{K}_{22} \mathbf{q}_2) (\mathbf{q}_1^T \mathbf{L}_1^T \mathbf{u})^2}{(\mathbf{q}_2^T \mathbf{K}_{12}^T \mathbf{q}_1)^2 (\mathbf{u}^T \mathbf{K}_0 \mathbf{u})} > 0. \quad (11.120)$$

This condition can be written in an alternative form as

$$\forall \mathbf{u} \exists \mathbf{q}_1 \forall \mathbf{q}_2 \quad (\mathbf{q}_2^T \mathbf{K}_{22} \mathbf{q}_2) (\mathbf{q}_1^T \mathbf{L}_1^T \mathbf{u})^2 > \beta_2 (\mathbf{q}_2^T \mathbf{K}_{12}^T \mathbf{q}_1)^2 (\mathbf{u}^T \mathbf{K}_0 \mathbf{u}) \quad (11.121)$$

for some $\beta_2 > 0$ and we see that it does not imply that $\mathbf{q}_1 \neq \mathbf{0}$ cannot belong to the null space of \mathbf{K}_{12}^T and, thus, does not guarantee that eq. (11.109) is fulfilled. Hence, both the conditions of eqs. (11.109) and (11.120) are required.

Summary. To ensure the solvability of the mixed problem the following conditions should be verified:

- For the two-field problem of eq. (11.88), we have to verify either (i) the *inf-sup* condition of eq. (11.95) or (ii) that the smallest eigenvalue for the eigenvalue problem of eq. (11.93) is greater than zero, and for the mesh size going to zero, it is still greater than zero.
- For the three-field problem of eq. (11.101), we have to verify either (i) the *inf-sup* conditions of eqs. (11.109) and (11.120), or (ii) that the smallest eigenvalues for the eigenvalue problems of eqs. (11.107) and (11.116) are greater than zero.

Moreover, we have to check that the constants in the *inf-sup* conditions, or the smallest eigenvalues, do not tend to zero for the diminishing element size.

Numerical *inf-sup* test. Two meshes were used; a regular mesh and a distorted mesh, of 2×2 , 4×4 , and 8×8 elements, see Fig. 11.7. Besides, two values of the Poisson ratio were used: $\nu = 0.3$ for a compressible material and $\nu = 0.4999$ for a nearly incompressible material.

For the HR5-S element, we solve the eigenvalue problem of eq. (11.93). For the HW14-SS, we solve the eigenvalue problem of eq. (11.116) and, instead of solving eq. (11.109), the pivots are controlled when calculating the inverse of

$$\begin{bmatrix} \mathbf{0} & \mathbf{K}_{12} \\ \mathbf{K}_{12}^T & \mathbf{K}_{22} \end{bmatrix} \quad (11.122)$$

and they are non-zero, which indicates that *Problem 1* is solvable.

The smallest eigenvalues γ for the HW14-SS element are shown in Fig. 11.8, where $N = 2, 4, 8$ is the number of subdivisions in one direction. The curves indicate that the discrete form of the *inf-sup* test is passed, thus the condition (11.114) is met. Note that identical curves were obtained for the HR5-S element.

For the regular meshes, the obtained curves are horizontal, similarly as for the 9/3 element shown in [17], Fig. 1, and for the MINI element shown in [46], Fig. 6. Both these elements have the property that there exists an analytical proof that they pass the *inf-sup* test and the corresponding numerical test is also passed. Hence, it is likely that the analytical *inf-sup* condition can also be verified for the HW14-SS element.

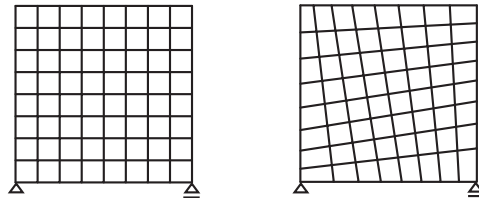


Fig. 11.7 *Inf-sup* test. Regular and distorted mesh of 8×8 elements.

11.5.1 Assumed stress HR elements: PS and HR5-S

In the class of the elements based on the HR functional, the PS element of [170] is standard. Currently, however, several other elements exist in the literature which perform slightly better for coarse distorted meshes; among them, the HR5-S element of [256]. Both these elements use the

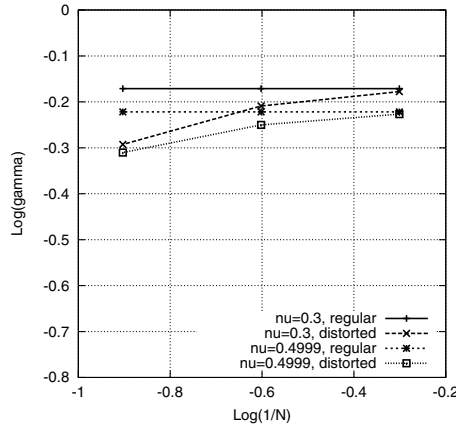


Fig. 11.8 Inf-sup test. Results for HW14-SS element. $E = 1$, $\nu = 0.3$ or 0.4999

same five-parameter representation of stress but in the PS element it is written using the natural coordinates, while in the HR5-S element the skew coordinates are used.

The early works on the HR elements, up to 1981, are reviewed in [223], while the more recent ones are reviewed in [256].

Assumed representation of stress. We use the contra-variant stress components σ^{kl} in the natural basis at the element’s center $\{\mathbf{g}_k^c\}$, i.e.

$$\boldsymbol{\sigma} = \sigma^{kl} \mathbf{g}_k^c \otimes \mathbf{g}_l^c, \quad k, l = 1, 2. \tag{11.123}$$

The components σ^{kl} are assumed and we denote the respective matrix as $\boldsymbol{\sigma}^\xi$. These components are transformed to the reference basis using

$$\boldsymbol{\sigma}^{\text{ref}} = \mathbf{J}_c \boldsymbol{\sigma}^\xi \mathbf{J}_c^T, \tag{11.124}$$

where \mathbf{J}_c is the Jacobian matrix evaluated at the element’s center of eq. (11.76).

The five-parameter representation of stress was already used by Pian in 1964 in [168] in Cartesian coordinates and later in [170] in the natural coordinates

$$\boldsymbol{\sigma}^\xi \doteq \begin{bmatrix} q_1 + q_2 \eta & q_5 \\ \text{sym.} & q_3 + q_4 \xi \end{bmatrix}. \tag{11.125}$$

This representation is symmetric, and includes the modes $\{1, \xi, \eta\}$ multiplied by five parameters q_i .

In [256], the above five-parameter representation of stress was written in the skew coordinates, i.e.

$$\boldsymbol{\sigma}^\xi \doteq \begin{bmatrix} q_1 + q_2 y_S & q_5 \\ \text{symm.} & q_3 + q_4 x_S \end{bmatrix} = \begin{bmatrix} q_1 + q_2 \eta + \underline{q_2 B \xi \eta} & q_5 \\ \text{sym.} & q_3 + q_4 \xi + \underline{q_4 A \xi \eta} \end{bmatrix}, \quad (11.126)$$

where A and B are defined below eq. (11.81). The bilinear (underlined) terms are non-zero only for irregular trapezoidal shapes, while they vanish for parallelograms. Still only five parameters q_i are used!

Verification of equilibrium equation for the assumed stress. For a single element, we can check whether the assumed representations of stresses satisfy the homogenous equilibrium equations. This property is not used in the construction of our elements, but it can be logically linked with their performance for characteristic shapes of the elements.

Note that in several papers, including [169, 170, 265], the satisfaction of the homogenous equilibrium equations is pivotal as they are appended to the HR functional via the Lagrange multiplier method. Then, however, the problem becomes more complicated, as the question of a suitable form of the Lagrange multiplier field arises (typically the incompatible displacement modes are exploited for this purpose). We stress that we do not use this approach.

We can check the equilibrium equations for some characteristic shapes of an element using a symbolic algebra. The homogenous equilibrium equations in the reference Cartesian coordinates, for a symmetric stress, are as follows

$$\frac{\partial \sigma_{xx}}{\partial x} + \frac{\partial \sigma_{xy}}{\partial y} = 0, \quad \frac{\partial \sigma_{xy}}{\partial x} + \frac{\partial \sigma_{yy}}{\partial y} = 0. \quad (11.127)$$

They are checked for the following specification of the stress components and their derivatives:

1. The stresses in the reference basis are obtained from the assumed representation $\boldsymbol{\sigma}^\xi$ using the transformation formula (11.124),

$$\boldsymbol{\sigma}^a \doteq \begin{bmatrix} \sigma_{xx} & \sigma_{xy} \\ \sigma_{xy} & \sigma_{yy} \end{bmatrix} = \mathbf{J}_c \begin{bmatrix} \sigma^{\xi\xi} & \sigma^{\xi\eta} \\ \sigma^{\xi\eta} & \sigma^{\eta\eta} \end{bmatrix} \mathbf{J}_c^T = \mathbf{J}_c \boldsymbol{\sigma}^\xi \mathbf{J}_c^T. \quad (11.128)$$

2. When the matrix $\boldsymbol{\sigma}^\xi$ is assumed in terms of the skew coordinates x_S, y_S , then, to enable numerical integration of the element, x_S, y_S are treated as functions of the natural coordinates ξ, η . Hence, we

can either use the chain rule of differentiation or directly express the derivatives w.r.t. x, y in terms of derivatives w.r.t. ξ, η as follows:

$$\begin{bmatrix} \frac{\partial \sigma}{\partial x} \\ \frac{\partial \sigma}{\partial y} \end{bmatrix} = \mathbf{J}^{-T} \begin{bmatrix} \frac{\partial \sigma}{\partial \xi} \\ \frac{\partial \sigma}{\partial \eta} \end{bmatrix}, \quad (11.129)$$

where $\sigma \in [\sigma_{xx}, \sigma_{yy}, \sigma_{xy}]^T$ is an arbitrary stress component in the form of eq. (11.126). Note that here \mathbf{J} is used, not \mathbf{J}_c .

The results of a verification of the equilibrium equation for the assumed stress are presented in Table 11.1, where “+” indicates that the equations are satisfied for an irregular shape of an element.

We see that, for the skew coordinates (HR5-S element), the equilibrium equations are satisfied point-wise, even for an irregular element. For the natural coordinates (PS element), they are satisfied point-wise only for parallelograms, while for irregular elements, only at the element’s center.

Table 11.1 Verification of equilibrium equation for the assumed stress.

σ^ξ assumed in	At arbitrary point	At center	Integral of eq. (11.127)
skew coordinates	+	+	+
natural coordinates	-(*)	+	-(*)

(*) satisfied only for parallelograms.

Verification of compatibility of the strains for assumed stresses. The compatibility condition for 2D strains is as follows:

$$\frac{\partial^2 \varepsilon_{xx}}{\partial y^2} + \frac{\partial^2 \varepsilon_{yy}}{\partial x^2} = 2 \frac{\partial^2 \varepsilon_{xy}}{\partial x \partial y}, \quad (11.130)$$

and we evaluate it for the strains calculated using the inverse constitutive matrix for the assumed stresses. We emphasize that we do not check the compatibility condition for the compatible strain but for the strains corresponding to (induced by) the assumed stress. They are obtained in the following steps:

1. The stresses in the reference basis are obtained as in eq. (11.128).
2. The strains corresponding to the assumed stresses are obtained from the inverse constitutive equation

$$\varepsilon_v = \mathbb{C}_{vv}^{-1} \sigma_v^a, \quad (11.131)$$

where $(\cdot)_v$ denotes a vector of components of a tensor (\cdot) , arranged in the order $\{xx, yy, xy\}$.

3. The skew coordinates x_S, y_S are treated as functions of the natural coordinates ξ, η . Hence, we can either use the chain rule of differentiation or directly express the first derivatives of strains w.r.t. x, y in terms of derivatives w.r.t. ξ, η as follows:

$$\begin{bmatrix} \frac{\partial \varepsilon}{\partial x} \\ \frac{\partial \varepsilon}{\partial y} \end{bmatrix} = \mathbf{J}^{-T} \begin{bmatrix} \frac{\partial \varepsilon}{\partial \xi} \\ \frac{\partial \varepsilon}{\partial \eta} \end{bmatrix}, \tag{11.132}$$

where $\varepsilon \in \{\varepsilon_{xx}, \varepsilon_{yy}, \varepsilon_{xy}\}$ is an arbitrary strain component. For the first derivatives of an arbitrary strain component, $\gamma \in \{\partial\varepsilon/\partial x, \partial\varepsilon/\partial y\}$, we similarly calculate the second derivatives,

$$\begin{bmatrix} \frac{\partial \gamma}{\partial x} \\ \frac{\partial \gamma}{\partial y} \end{bmatrix} = \mathbf{J}^{-T} \begin{bmatrix} \frac{\partial \gamma}{\partial \xi} \\ \frac{\partial \gamma}{\partial \eta} \end{bmatrix}, \tag{11.133}$$

where

$$\frac{\partial \gamma}{\partial x} = \left\{ \frac{\partial^2 \varepsilon}{\partial x^2}, \frac{\partial^2 \varepsilon}{\partial y \partial x} \right\}, \quad \frac{\partial \gamma}{\partial y} = \left\{ \frac{\partial^2 \varepsilon}{\partial x \partial y}, \frac{\partial^2 \varepsilon}{\partial y^2} \right\}, \tag{11.134}$$

and they contain all the second derivatives needed in eq. (11.130).

Note that \mathbf{J} is used here not \mathbf{J}_e .

The results of the verification of the compatibility condition are presented in Table 11.2, where “+” indicates that the equations are satisfied for an irregular shape of an element.

We see that, for the skew coordinates (HR5-S element), the compatibility condition is satisfied, even for irregular elements, while for the natural coordinates (PS element), the compatibility condition is satisfied only for parallelograms.

Table 11.2 Verification of the compatibility condition for the assumed stress.

σ^ξ assumed in	At arbitrary point	At center	Integral of eq. (11.130)
skew coordinates	+	+	+
natural coordinates	-(*)	-(*)	-(*)

(*) satisfied only for parallelograms.

Remark. We have earlier shown that the natural coordinates cannot be treated as being associated with the natural basis at the element's center, as this leads to the "fictitious" parallelogram element shown in Fig. 11.6. The above tests of the homogenous equilibrium equation and of the compatibility of strains equation provide another argument that it is more rational to assume the representation of stress in terms of the skew coordinates than in the natural coordinates.

We do not exploit this property in the elements' formulation in any particular way. Nonetheless, the numerical results indicate that the accuracy of elements depends on the coordinates used for the stress representation.

Assumed stress elements: PS and HR5-S. The assumed stress elements are developed from the two-field HR functionals in the basic non-enhanced form of eqs. (11.4) and (11.7). In these functionals, \mathbf{u} is the compatible field while $\boldsymbol{\sigma}$ is the assumed field of the form

$$\boldsymbol{\sigma}^a = \mathbf{J}_c \boldsymbol{\sigma}^\xi \mathbf{J}_c^T, \quad (11.135)$$

which is the transformation rule for the contra-variant components of a tensor of eq. (11.124). Besides, in $\boldsymbol{\sigma}^\xi$ we use the 5-parameter stress of eq. (11.125) for the PS elements, or of eq. (11.126) for the HR5-S element. The increment of the assumed stress has the analogous form, where $\Delta\boldsymbol{\sigma}^\xi$ has the structure of $\boldsymbol{\sigma}^\xi$ of eq. (11.125), but the multipliers q_i are replaced by Δq_i .

In the HR functionals, we use the reduced constitutive operator for the plane stress condition \mathbb{C}^* of eq. (7.64).

The PS element is a standard in the class of mixed HR elements, but the HR5-S element performs slightly better for coarse distorted meshes. Its formulation is very simple and it yields results similar to these by the 5β -A,B,C elements of [265] and the QE2 element of [177], which are more complicated and use more parameters.

Remark. The discrete HR functional depends on two sets of variables: the nodal displacements \mathbf{u}_I and the elemental stress multipliers \mathbf{q} . The obtained set of FE equations is given by eq. (11.27) and the scheme U2 of eq. (11.34) should be used to update the stress multipliers. Consider the non-reduced tangent matrix of eq. (11.27). At $(\mathbf{u} = \mathbf{0}, \mathbf{q} = \mathbf{0})$, the sub-matrix \mathbf{K} is equal to zero and we obtain

$$\begin{bmatrix} \mathbf{0} & \mathbf{L} \\ \mathbf{L}^T & \mathbf{K}_{qq} \end{bmatrix}, \quad (11.136)$$

for which the linear element is very efficient.

Remark. Assumed stress/enhanced strain elements. The HR element can also be developed for the seven-parameter representation of stresses, but this element is too stiff, no matter in which coordinates the stresses are written. Hence, the HR functional must be enhanced and two additional EAS or EADG modes were used in the HR9 element in [256]. The HR9 element performs identically as the HR5-S element, but is less efficient. However, it still can be used in 2D and shell elements with drilling rotations, for which this type of enhancement is beneficial, see Sect. 12.

11.5.2 Assumed stress and strain HW14-SS element

The main difference between the HR elements and the HW elements is that strains are retained in the latter and we have to select their representation.

Generally, the strain representation analogous to that used for stress is too poor. A better one is implied by the inverse constitutive equation

$$\begin{bmatrix} \varepsilon_{11} \\ \varepsilon_{22} \\ \varepsilon_{12} \end{bmatrix} = \begin{bmatrix} c_1 & c_2 & 0 \\ c_2 & c_1 & 0 \\ 0 & 0 & c_3 \end{bmatrix} \begin{bmatrix} q_1 + q_2\eta \\ q_3 + q_4\xi \\ q_5 \end{bmatrix} = \begin{bmatrix} (c_1q_1 + c_2q_3) + c_1q_2\eta + c_2q_4\xi \\ (c_2q_1 + c_1q_3) + c_2q_2\eta + c_1q_4\xi \\ c_3q_5 \end{bmatrix}, \quad (11.137)$$

where the five-parameter representation of stress of eq. (11.125) and a typical structure of the inverse constitutive matrix are used. This suggests that a seven-parameter representation of strain should be used; constant representation for ε_{12} and linear representations for ε_{11} and ε_{22} . However, if ε_{12} is additionally enhanced by two modes, then the accuracy for coarse distorted meshes improves. Further improvement is obtained if this representation of strain is assumed in terms of the skew coordinates of eq. (11.81).

Assumed representation of strain. The covariant components of strain are assumed in the co-basis $\{\mathbf{g}_c^k\}$, i.e.

$$\boldsymbol{\varepsilon} = \varepsilon_{kl} \mathbf{g}_c^k \otimes \mathbf{g}_c^l. \quad (11.138)$$

The matrix of components $\varepsilon_{\alpha\beta}$ can be designated as $\boldsymbol{\varepsilon}_\xi$ and transformed to the ortho-normal reference basis by using

$$\boldsymbol{\varepsilon}^{\text{ref}} = \mathbf{J}_c^{-T} \boldsymbol{\varepsilon}_\xi \mathbf{J}_c^{-1}. \quad (11.139)$$

The scalar product of the assumed representations of stress and strain, eqs. (11.124) and (11.139) is invariant, which implies invariance of the derived elements.

The assumed nine-parameter representation of strain is

$$\boldsymbol{\varepsilon}_\xi \doteq \begin{bmatrix} q_6 + q_7 y_S + q_8 x_S & q_{12} + q_{13} x_S + q_{14} y_S \\ \text{sym.} & q_9 + q_{10} x_S + q_{11} y_S \end{bmatrix}, \quad (11.140)$$

where each component is a linear polynomial of x_S and y_S . We see that this representation consists of two parts,

$$\boldsymbol{\varepsilon}_\xi = \begin{bmatrix} q_6 + q_7 y_S & q_{10} \\ \text{sym.} & q_8 + q_9 x_S \end{bmatrix} + \begin{bmatrix} q_{11} x_S & q_{13} x_S + q_{14} y_S \\ \text{sym.} & q_{12} y_S \end{bmatrix}, \quad (11.141)$$

where the first part is analogous to the five-parameter representation of eq. (11.126) used for stress, while the second part is analogous to the four-parameter representation of the EAS method, see eq. (11.62), but written in the skew coordinates.

Compatibility of assumed strains. The compatibility condition for 2D strains is given by eq. (11.130). Note that, for the HR element, we verified the compatibility of the strains calculated for assumed stresses, while here we verify the compatibility of the assumed strain. Hence, we can skip point 1 of the previously defined procedure. Results of the test of the compatibility condition for the strain of eq. (11.140) are presented in Table 11.3, where “+” indicates that the condition is satisfied for an element of an arbitrary irregular shape.

Table 11.3 Verification of the compatibility condition for the assumed strain.

$\boldsymbol{\varepsilon}_\xi$ assumed in	At arbitrary point	At center
skew coordinates	+	+
natural coordinates	-(*)	-(*)

(*) satisfied only for parallelograms.

We see that for the representation in the skew coordinates, the compatibility condition is satisfied point-wise, even for irregular elements. When the strain is written in natural coordinates, then this equation is only

satisfied for parallelograms. This provides the argument that it is more rational to assume the representation of strain in the skew coordinates than in the natural coordinates.

Element HW14-SS. The assumed stress/assumed strain element is developed from the three-field HW functionals in the basic non-enhanced form of eqs. (11.1) and (11.3). The compatible displacement \mathbf{u}^c is defined in eq. (11.14). The independent stress $\boldsymbol{\sigma}$ and the independent strain $\boldsymbol{\varepsilon}$ are constructed as the assumed fields. The assumed fields are constructed as follows:

1. The assumed stress is constructed similarly as for the HR5-S element,

$$\boldsymbol{\sigma}^a = \mathbf{J}_c \boldsymbol{\sigma}^\xi \mathbf{J}_c^T, \quad (11.142)$$

using the transformation rule of eq. (11.124) and the five-parameter representation of $\boldsymbol{\sigma}^\xi$ of eq. (11.126). Recall that for this representation, the equilibrium equations are satisfied point-wise, even for an irregular element, see Table 11.1.

2. The assumed strain is constructed as

$$\boldsymbol{\varepsilon}^a = \mathbf{J}_c^{-T} \boldsymbol{\varepsilon}_\xi \mathbf{J}_c^{-1}, \quad (11.143)$$

using the transformation rule of eq. (11.139) for the covariant components of a tensor. The nine-parameter strain representation of $\boldsymbol{\varepsilon}_\xi$ is given by eq. (11.140) and it satisfies the compatibility condition.

We designate this element as HW14-SS because it has 14 modes and both the stress and strain representations are assumed in skew coordinates.

In numerical tests, the HW14-SS element performs identically as the HR5-S element, i.e. is slightly more accurate and less sensitive to mesh distortion than the PS element and the enhanced strain elements (ID4, EAS4, EADG4).

The HW14-SS element uses a smaller number of modes than other HW elements described in the literature, such as the QE2 element of [177] with 16 modes, and the elements with 22 modes \bar{B} -QE4 of [178] and $\bar{B}(x, y)$ -QE4 and $\bar{B}(\xi, \eta)$ -QE4 of [176], but its accuracy is identical.

Remark 1. If we use less parameters for the assumed strain, e.g., seven instead of nine, then it is beneficial to use the covariant instead of contravariant representation of strain. The results for the element based on the nine-parameter representation of strain are not altered by this change.

Remark 2. Assumed stress and strain/enhanced strain elements. The HW element can also be developed for the seven-parameter representation of stresses and the nine-parameter representation of strain, but must be enhanced; two additional EADG modes are used in the HW18 element in [257]. This element performs identically to the HR14-SS element, but is less efficient. However, it can still be used in 2D+drill and shell elements, for which the EAGD enhancement is particularly beneficial, see Sect. 12.

Remark 3. The discrete HW functional depends on two sets of variables: the nodal displacements \mathbf{u}_I and the elemental stress and strain multipliers \mathbf{q} . The obtained set of FE equations is given by eq. (11.27) and to update the stress and strain multipliers, the scheme U2 of eq. (11.34) should be used. Consider the non-reduced tangent matrix of eq. (11.27). Several sub-matrices of it are equal to zero at $(\mathbf{u} = \mathbf{0}, \mathbf{q} = \mathbf{0})$, and we obtain

$$\begin{bmatrix} \mathbf{K} & \mathbf{L} \\ \mathbf{L}^T & \mathbf{K}_{qq} \end{bmatrix} = \begin{bmatrix} \mathbf{K} & \mathbf{L}_1 & \mathbf{L}_2 \\ \mathbf{L}_1^T & \mathbf{K}_{11} & \mathbf{K}_{12} \\ \mathbf{L}_2^T & \mathbf{K}_{12}^T & \mathbf{K}_{22} \end{bmatrix} \rightarrow \begin{bmatrix} \mathbf{0} & \mathbf{L}_1 & \mathbf{0} \\ \mathbf{L}_1^T & \mathbf{0} & \mathbf{K}_{12} \\ \mathbf{0} & \mathbf{K}_{12}^T & \mathbf{K}_{22} \end{bmatrix}, \quad (11.144)$$

where 1 designates the q_i parameters for stress, and 2 designates the q_i parameters for strain. The presence of zero sub-matrices can be used to obtain a very efficient linear version of this element.

11.6 Modification of $\mathbf{F}^T \mathbf{F}$ product

We can modify the $\mathbf{F}^T \mathbf{F}$ product in the Green strain in the way which preserves a correct rank of the elements and improves their coarse mesh accuracy. The deformation gradient \mathbf{F} is expanded in the Taylor series w.r.t. the natural coordinates at the element's center, and the $\mathbf{F}^T \mathbf{F}$ product is approximated as follows:

$$\mathbf{F}^T \mathbf{F} \approx \mathbf{F}_c^T \mathbf{F}_c + \mathbf{A} + \mathbf{A}^T, \quad (11.145)$$

where

$$\mathbf{A} \doteq \mathbf{F}_c^T \left[\underline{\xi(\mathbf{F}, \xi)_c + \eta(\mathbf{F}, \eta)_c + \xi\eta(\mathbf{F}, \xi\eta)_c} + \frac{1}{2}\xi^2(\mathbf{F}, \xi\xi)_c + \frac{1}{2}\eta^2(\mathbf{F}, \eta\eta)_c \right]. \quad (11.146)$$

In other words, the Taylor expansion is combined with a selection of meaningful terms in the product. A correct rank of the reduced tangent matrix

\mathbf{K}^* in eq. (11.30) is yielded by the first three (underlined) linear and bilinear terms of \mathbf{A} , while the last two quadratic terms of \mathbf{A} are needed to pass the patch test.

The concept of expansion was proposed in [135] and was later used in several papers, including [132], but the terms selected in these works are different from these in eq. (11.145).

1. The under-integrated and gamma-stabilized elements were developed in [135] and the following expansion was used:

$$\varepsilon(\xi, \eta) = \mathbf{B}(\xi, \eta) \mathbf{u}_I, \quad \mathbf{B}(\xi, \eta) \approx \mathbf{B}_c + \xi(\mathbf{B}_{,\xi})_c + \eta(\mathbf{B}_{,\eta})_c, \quad (11.147)$$

where \mathbf{B} is the strain-displacement matrix, see eq. (2.5a) therein. This formula corresponds to the first two of the three underlined terms in eq. (11.146).

2. In [132], the following terms of the Taylor series were selected,

$$\begin{aligned} \bar{T}(f) \doteq & \xi(f_{,\xi})_c + \eta(f_{,\eta})_c + \xi\eta(f_{,\xi\eta})_c \\ & + \frac{1}{6} [\xi^3(f_{,\xi\xi\xi})_c + \eta^3(f_{,\eta\eta\eta})_c + 3\xi^2\eta(f_{,\xi\xi\eta})_c + 3\eta^2\xi(f_{,\eta\eta\xi})_c], \end{aligned} \quad (11.148)$$

and applied to the “stabilizing” strain and the “enhancing” strain field, see eqs. (23) and (24) therein. We see that the expansions of eqs. (11.148) and (11.145) are different in the higher-order terms.

Another difference is that small strains are used in both of the cited papers, so the term $\mathbf{F} + \mathbf{F}^T$ was modified, while we modify the product $\mathbf{F}^T \mathbf{F}$ as we use the Green strain.

A full set of tests for the EADG4, HR5-S, and HW14-S elements is given in [257]. For the mixed elements, HW14-S and HR5-S, the expansion was applied to \mathbf{F} , as given by eq. (11.145), while for the EADG4 element, we expanded the whole enhanced deformation gradient, $\mathbf{F} + \tilde{\mathbf{H}}$, where $\tilde{\mathbf{H}}$ is defined by eq. (11.71). The modification of the $\mathbf{F}^T \mathbf{F}$ product was proved to be beneficial in the case of coarse distorted meshes.